SHORT RANGE DISPERSION OF SULFUR DIOXIDE FROM A SMELTER COMPLEX

APRIL, 1979

SHORT RANGE DISPERSION OF SULFUR DIOXIDE FROM A SMELTER COMPLEX

Minnesota Environmental Quality Board
Regional Copper-Nickel Study
Author: G. William Endersen
April 1979

SHORT RANGE DISPERSION OF SULFUR DIOXIDE FROM A SMELTER COMPLEX

INTRODUCTION

Sulfur dioxide from a smelting operation would be released primarily as uncollected fugitive emissions from the smelter building and as stack emissions of weak gas streams collected by hooding and tail gases from the acid plant (see volume 2, chapter 4).

Four representative cases of smelter design and emissions control were developed to characterize the range of potential SO_2 emission impacts. The Base Case assumes a flash smelter/refinery complex producing 100,000 MTPY (metric tons per year) of copper and nickel with good secondary hooding to collect weak SO_2 gas streams that are then sent directly to the stack. That portion of the weak gas streams which escapes collection by the hood system is released to the environment as low level emissions commonly referred to as "fugitive emissions". The strong gas stream is treated by a double contact sulfuric acid plant to reduce its SO_2 content to 650 ppm (parts per million) before being sent to the stack.

The High Fugitive Basic Model is the same as the Base Case but has no secondary hooding for collection of the weak gas streams. Thus, a larger amount of SO_2 would be allowed to escape directly from the building as fugitive emissions, rather than be diverted to the stack, but the total SO_2 release would be the same in either case. The Option 1 case is similar to the Base Case, but includes a tail gas scrubber in addition to the acid plant. The Option 2 case involves good hooding for the weak SO_2 streams and treatment in a scrubber (with 90% SO_2 removal) of both the weak gas stream and the tail gas stream from the acid plant. Table 1 presents the model annual SO_2 emissions for these four cases. Here it is assumed that the smelter will operate normally for 350 days per year. Therefore, the

average emission rate in gm/sec for the long term model, which assumes constant operation throughout the year, will be less than that for the short term models for normal operations. Stack and fugitive SO_2 emissions rates for short and long term models are summarized in Table 2. Emissions during periods of upset are discussed later. These cases and the mechanisms for potential SO_2 release, as well as the large uncertainties associated with the emission rates, are discussed in detail in the Technical Assessment section, volume 2, chapter 4.

The physical features of the smelter, for dispersion modeling purposes, are assumed to be as follows during normal operation:

Building length	152 m
Building width	122 m
Building height	50 m
Stack height	60 m
Stack internal diameter	2.2 m
Exit gas velocity	22 m/sec
Exit gas temperature	82°C

The relatively low stack height represented by the use of the value of 60 m seems to be typical of new smelters. Although the stack is only 10 m taller than the smelter building, physical separation of the stack from the building and a sufficiently high exit velocity should prevent aerodynamic downwash of the stack plume caused by the building wake. The 22 m/sec exit velocity is much higher than that of most existing smelters. The value was selected to avoid stack downwash by using the value of 1.5 times the 95th percentile of wind speed measured at Hibbing and adjusted to 50 m under neutral stability by the formulation shown in Table 3. Neutral stability was used because it is the usual stability under strong winds.

The computation of ambient SO_2 concentrations from these model smelters allows: 1) comparison of computed concentrations with values specified by ambient standards and Prevention of Significant Deterioration (PSD) allowable increments; 2) estimation of deposition rates; and 3) identification of potential concentrations and loading rates leading to physical and biological impacts for various degrees of emission control. Time periods of concern for these impacts include both short term (3 and 24 hours) and long term (1 year).

Dispersion models applied to a non-site specific smelter must be significantly general that the results can be applied to a number of different potential smelter sites. The Study Region of northeastern Minnesota can be characterized as mostly flat to moderately rolling with the exception of the Giants Range (see topography discussion in volume 3, chapter 1). Areas on and adjacent to the Range are characterized by enhanced mechanical turbulence, airflow channeling, plume impingement on terrain features, and downslope drainage flow as compared to the remainder of the Region. The approach taken toward modeling a potential smelter in this region, for both short term and long term averages, has been to model plume dispersion over gently rolling, uncomplicated terrain and to use those results to describe dispersion over the majority of the Study Area. These results would not apply where local topography produces major changes in the dispersion patterns. For example, specific analyses would have to be performed for any proposed smelter site where the plume could impact elevated terrain (such as the Giants Range), where plume dispersion could be hindered by the sides of a valley or by an inversion capping the cold air in the valley in the morning, or where the plume would have become stable by transport over water. A brief discussion of plume dispersion mechanisms and smelter siting considerations for various areas of northeastern Minnesota is presented in the Appendix to this report.

Dispersion Models

Short Term (3 and 24-hour) averages

The best approach to dispersion modeling for gently rolling terrain with no specific designated source location is to employ steady state Gaussian models. The USEPA considers Gaussian models to be state-of-the-art for estimating concentrations of SO_2 and particulate matter and recommends them for most point source applications (USEPA, 1978).

Accuracy within a factor of two (that is, actual maximum concentrations ranging from 50% to 200% of the computed concentrations) has frequently been claimed for Gaussian modeling. A recent position paper by the American Meteorological Society Committee on Atmospheric Turbulence and Dispersion (1978) expressed the opinion that the factor of two error range is probably realistic for practical point source Gaussian modeling using good meteorological data and in the absence of certain conditions. Those important conditions under which a significantly larger error could be expected include the following:

1) aerodynamic wake flow, including building and terrain wakes and stack downwash
2) buoyant effluent release
3) flows over surfaces other than flat to gently rolling open fields, such as cities, water, rough terrain and forests
4) dispersion in extremely stable or extremely unstable conditions
5) dispersion at downwind distances greater than 10-20 km

It is also useful for interpretation and evaluation if the models are widely known and used by the scientific community. The Texas Episodic Model (TEM) (Christiansen, 1976) and Climatological Dispersion Model (CDM) (Busse and Zimmerman, 1973; Brubaker, et al., 1977) are both widely used and have been recom-

mended by the USEPA (1978). Therefore, these two dispersion models were chosen for estimating the short range ground level concentrations caused by emissions from the smelter stack. A less widely-known model, a modified version of a building source model developed by the H.E. Cramer Co., was employed to estimate the dispersion of fugitive emissions (Cramer, et al., 1975).

Short Term Averages

The Texas Episodic Model was used to estimate short term (3 and 24-hour) ambient concentrations. TEM computes plume rise by the Briggs (1969) method and adjusts input wind speed from an assumed height of 10 m to stack height by the stability-dependent method used in CDM (Busse and Zimmerman, 1973). The plume can reflect off the ground and the mixing lid.

Pollutants can be lost from the plume by chemical conversion, dry deposition and wet deposition. The combined effect of these mechanisms is termed "pollutant decay". Chemical conversion and dry deposition effects are included in TEM through an exponential decay term. Chemical conversion of SO_2 in the plume is estimated to occur at a rate of 0.5% per hour. Dry deposition rates for SO_2 were estimated with a surface depletion model using deposition velocities of 0.2 and 0.8 cm/sec over snow and no snow, respectively (Garland, 1977). The dry deposition was assumed to occur through a plume of 220 m average thickness (twice the typical effective plume height) from the source to 10 km downwind. No wet deposition (pollutant removal by precipitation) was considered in the short term worst case computations.

Stability-dependent SO_2 half-lives for snow and no snow are listed in Table 4. These half-lives are long enough that SO_2 concentrations are decreased significantly by SO_2 decay within 10 km of the source only under very light wind

conditions, when the model does not do a very good job anyway.

Dispersion coefficients are those from Turner (1970). Computed concentrations within the model are for 10-minute intervals, the time period for which the Turner curves were developed. These values are then adjusted internally to estimate 3-hour averages by the stability-dependent method from Singer (1961). 24-hour averages are computed by combining 8 3-hour meteorological scenarios. TEM results were computed to 10 km from the smelter. The accuracy of the model deteriorates significantly beyond 10 km.

Modeling the dispersion of fugitive emissions requires a somewhat different Gaussian approach. Building-induced turbulence tends to mix fugitive emissions on the downwind side of the building. This "cavity effect" dilutes the plume at the source and produces a ground level neutrally buoyant plume of some initial size. The short term fugitive emissions dispersion model utilized in this study was adapted from a building release model developed by the H.E. Cramer Co. (Cramer, et al., 1975).

The initial size of the plume is incorporated into the dispersion computations by giving it initial standard deviations σ_{yo} and σ_{zo} at the source as follows:

$$\sigma_{yo} = \frac{y_o}{4.3}$$

$$\sigma_{zo} = \frac{H_B}{2.15}$$

where y_o = building crosswind dimension

H_B = building height

For simplicity, y_o was assumed to be building length, 152 m, in all computations. Therefore, the values are the following:

$$\sigma_{yo} = \frac{152 \text{ m}}{4.3} = 35 \text{ m}$$

$$\sigma_{zo} = \frac{50 \text{ m}}{2.15} = 23 \text{ m}$$

Computationally, this initial dispersion is included in each model run as stability-dependent virtual distances from Turner's curves corresponding to each y_o and z_o value. Dispersion coefficients incorporated into the model are based on the Pasquill-Gifford curves (Pasquill, 1961, and Gifford, 1961) because the strict Cramer version requires rather sophisticated meteorological data not available for the Study Region. The use of the Pasquill-Gifford curves produces concentrations smaller than those for the Cramer version during unstable conditions and larger than for the Cramer version at far downwind distances during neutral and stable conditions. Sample times are adjusted from 10 minutes to one hour by multiplying all concentrations by 0.70 as recommended by Turner (1970).

In a second modification, the effective height of emission was considered to be the building height rather than ground level. The H.E. Cramer Co. has reported that a building height release yields a better fit to the scant existing data than does surface release (Bowers, 1977).

Wind speeds were adjusted from the Flight Service Station 6.4 m measuring height to building height by a formulation similar to that used in CDM (see Table 3). The only difference is in the values for p, which differ slightly for stability class F.

Physical and chemical pollutant decay were computed as for TEM, but were limited to an estimated plume depth of 100 m. SO_2 half-lives for the Fugitive Model are the same as those used in the TEM (Table 4).

The plume can experience multiple reflections at the ground and mixing lid.

The H.E. Cramer model for building releases has not been as widely used as has TEM, and possibly has never before been utilized with these modifications. Therefore, it is difficult to estimate its validity. From knowledge of the dispersion coefficients, it is felt that the Fugitive Model may be too conservative (that is, computed concentrations may significantly exceed actual levels) at longer distances, such as near the 10 km modeling limit. The model is also invalid very close to the source (approximately the first few hundred meters) because of the initial dispersion approximation. The near-source error is by far the largest for very stable flow which, in the mathematical treatment, is not mixed to the surface in high enough concentrations sufficiently close to the source to approximate the actual situation. Otherwise, for conditions near neutral stability, the Fugitive Model probably also has factor of two accuracy except near major terrain features.

Another limitation of the fugitive model is that it cannot deal with a ground plume's tendency to follow the valleys and impact on hillsides. In addition to direct impaction, valleys can produce high concentrations by limiting dispersion. They can also steer the ground plume away from the path of the elevated stack plume.

Long Term Averages

Long term averages were estimated with the very widely used Climatological Dispersion Model (Busse and Zimmerman, 1973). CDM uses annual wind and stability complications to compute 22.5° sector average pollutant concentrations. Vertical dispersion coefficients are from the standard Pasquill-Gifford curves (Pasquill, 1961, and Gifford, 1961). Plume rise is from

Briggs (1969). Wind speeds are adjusted to stack height by a stability-dependent relationship (see Table 3).

CDM was adapted for fugitive emission dispersion by using an emission height of 50 km (building height), a very low exit velocity of 1 m/sec, a very wide stack diameter of 10 m and a low exist gas temperature of 40°C. This scheme artificially lowers the fugitive contribution very close to the source, but probably is reasonable beyond about a kilometer, depending on stability. Validity near the source decreases with increasing stability.

Long term modeling calls for the inclusion of wet as well as dry deposition effects. Pollutants can be taken up by cloud droplets and then deposited on the surface when the droplets become large and precipitate (washout). They can also be removed through capture by falling raindrops or, less efficiently, by snowflakes (rainout). These two precipitation removal effects were included in the decay term by assuming a precipitation event once every 1.9 days during the rain season and every 4.0 days during the snow season (Watson, 1978). The snow season was considered to be from November 1 to April 15 (5½ months) on the average, and precipitation removal was combined with chemical decay and seasonally-weighted dry deposition for both stack and fugitive emissions. These removal totals were weighted for 92% stack and 8% fugitive emissions from the Base Case (see Table 1). This computation led to an annual average SO_2 half-life of 10.3 hours. Seasonal variations were from 5.8 hours during the summer to 15.6 hours during the winter. The total effect of chemical decay, dry deposition and wet deposition was to decrease the computed average annual SO_2 concentrations by only about 4% at 10 km. Nearer to the source, the percentage decrease in concentrations due to removal would obviously be smaller.

Meteorological Input Data

Meteorological input data for the 24-hour dispersion model runs were selected from data collected at the Federal Aviation Administration Flight Service Station at the Hibbing Airport during 1976-1977. Because of the probable low release heights from the smelter, worst case dispersion days (that is, those days causing the highest ground level concentrations) were selected on the basis of wind persistence and lack of precipitation.

Days during which the wind direction varies through only a small compass angle (less than about 40°) are not at all uncommon, and most occur during the cold season with steady northwesterly sinds. Winds are generally less persistent in the summer and are more likely to become calm at night. Eight days were selected for modeling because of their very persistent winds. They can be considered representative of typical worst case days for ambient ground level concentrations of pollutants released from a model smelter and are similar to days likely to occur during any year. These days are as follows:

March 14, 1976
July 23, 1976
October 28, 1976
November 6, 1976
December 20, 1976
January 15, 1977
February 28, 1977
October 30, 1977

Wind speed, wind direction and temperature data were taken directly from the Hibbing Flight Service Station hourly data record. Hourly mixing depths were estimated from the hourly data with some guidance from Holzworth (1972). Stability classes were estimated by combining the objective Turner method with insight gained through analysis of the additional data available. Input

data for each of the 8 days, averaged into 3-hour periods for TEM, are listed in Tables 5-12.

The input meteorological data set for CDM is the 1976 STAR tabulation (joint frequency table of stability, wind direction, and wind speed) for Hibbing. Seasonal tabulations were not available. Average afternoon and nocturnal mixing heights were estimated to be 1200 and 460 m, respectively, and a mean annual temperature of 2°C was input.

Short Term Results

24-hour modeling results

The eight days listed in the previous section were run on both the TEM and Fugitive models with Base Case SO_2 emission rates. Concentration isopleths for the stack emissions for each day are presented in Figures 1 through 8. Maximum concentrations from the stack emissions alone range from 33 to 55 $\mu g/m^3$ SO_2 and occurred at distances of 3.25 to 5.1 km downwind. The patterns, as expected, indicate that maximum impacts would occur closer to the source during the warm season when the atmosphere is generally more unstable and turbulent than during the cold season.

The magnitude of these maximum impacts, however, seems to be dependent mainly on wind persistence rather than atmospheric stability. A careful examination of 1976-1977 meteorological data collected at the Hibbing Airport Flight Service Station clearly showed a much larger diurnal variation in wind direction during summer than during winter. The greater wind persistence during the cold season yielded many more worst case dispersion days during that part of the year. Cold season plumes would generally be stable to slightly unstable and produce narrow areas of impact. Worst case dispersion days occasionally occur during the warm season and could produce 24-hour

maximum concentrations of stack emissions similar to those during winter.

The warm season area of impact, as typified by the 23 July 1976 isopleths, (Figure 2), would be much broader than that for the cold season, however, because of the generally more variable wind direction and enhanced dispersion during summer.

Modeled fugitive SO_2 concentrations for these days are presented in Figures 9 through 16. Concentrations would be highest immediately adjacent to the smelter building and then decrease exponentially with distance from the source. As with the stack contribution, the area of impact would be broadest on sunny summer days when downwind dispersion is most rapid.

Figures 17 through 24 are plots of maximum 24-hour concentrations with distance for the stack, fugitive and total SO_2 for the Base Case on the eight days. Plots are of computed levels from 0.25 to 10.0 km from the source, the approximate range of model validity. An implicit assumption in computing this total by simple addition is that the wind is constant with height in the low levels so that the stack and fugitive plumes parallel each other. Low level wind shear could cause the two plumes to be transported in different directions, resulting in lower maximum concentrations and broader areas of impact.

The plots of maximum SO_2 with distance all have several basic features. Concentrations decrease rapidly downwind from a peak value on the lee of the smelter building resulting from fugitive emissions. Concentrations then increase again to a maximum value in the 1 to 4 km downwind range as the stack release becomes the dominant component of the total. Beyond this peak value, the concentrations decrease more gradually with distance

and continue to be dominated by the stack emissions. The downwind concentration decrease would be most rapid during summertime unstable conditions and most gradual during wintertime stable and neutral conditions.

The Class I and Class II 24-hour (PSD) Prevention of Significant Deterioration allowable SO_2 increments of 5 and 91 $\mu g/m^3$, respectively (see section 3.2.3 of volume 3, chapter 3) are also indicated on Figures 17 through 24. Computed concentrations for all eight worst cases greatly exceed the Class I increment at all distances out to 10 km. However, six of the eight cases modeled yielded values which remain below the Class II increment at all distances beyond 0.25 km and the remaining two cases exceed it only very close to the source. The computed downwind peaks range from 49 to 89 $\mu g/m^3$. The presence of the nominal factor of two error in the modeling plus the possibility of the occurrence of a day with even greater wind persistence indicate that concentrations in excess of the Class II increment might easily occur, based on the modeling results presented here.

The two days with the highest computed 24-hour SO_2 concentrations, excluding those high levels adjacent to the smelter, were 23 July 1976 and 30 October 1977 with maxima of 89 and 80 $\mu g/m^3$, respectively. Maximum ground level concentrations from 0.25 to 10.0 km were also computed for these two days using the Option 1 model, High Fugitive Basic Model and the Option 2 model discussed earlier (Tables 1 and 2). The results are presented in Figures 25 through 30. The High Fugitive Basic Model computations show exceedances of both the Class I and Class II PSD increments from the source to beyond 10 km for 23 July 1976 and to about 7.3 km for 30 October 1977. The stack emissions make only a very small contribution to the total concentration for this model smelter case.

The Option 1 and 2 results are much lower than the High Fugitive Basic

concentrations, with the Option 2 model producing computed concentrations lower than those for the Option 1 model. Both resulted in lower concentrations than did the Base Case model, were below the Class II increment at all but very short distances from the smelter, and were above the Class I increment at all distances to 10 km.

The dates selected for worst case computations had wind directions that are, of course, reflected in the concentration isopleths. Actual smelter plumes could be transported in any direction with a likelihood shown by the wind roses (Watson, 1978 b.) The annual Hibbing wind rose is included here (Figure 31). Northwest and southeast are obviously the most frequent wind directions. Worst cases are most likely to occur along directions of maximum wind persistence. Figure 32 represents wind persistence based on data collected at Hibbing Airport during the period November 1, 1976 through October 31, 1977. The radial scale represents the number of successive hours that the wind blew from a given direction on the 36-point compass. Isopleths have been drawn to represent the frequency of these occurrence during that period. For example, the wind persisted from the north (360°) for at least 10 hours approximately 13 times, but rarely or never persisted for 10 hours from the west. Winds from the north-northwest and south had the greatest persistence and would likely produce the highest 24-hour concentrations to the south-southeast and north of the smelter, respectively.

3-hour modeling results

Eleven hypothetical cases were developed to include the range of 3-hour stability conditions, wind speeds, temperature, and mixing heights typical of northern Minnesota (see Table 13). All eleven cases were run with the Texas Episodic Model and Fugitive Model with Base Case stack and

Fugitive emissions. Plots of the worst case (i.e., highest peak concentrations) for each basic stability class (cases 1, 3, 9, 10 and 11) are present in Figures 33 and 37. Maximum downwind concentration peaks, beyond the near-source high concentration region, and their downwind distances are listed in Table 14.

The downwind concentration patterns are strongly related to stability class. Figure 33 illustrates the SO_2 concentrations that could result under unstable class B conditions. The concentration is at its highest level near the smelter as a result of the fugitive emissions. Concentrations decrease rapidly downwind as the fugitive emissions disperse and increase again to a peak value where the stack plume reaches the ground in significant amounts. Active mixing in the unstable lower layers continues the rapid decrease in concentration with distance.

As shown by the plots (Figures 33 through 37), increasing atmospheric stability causes the distance to the maximum downwind peak to increase dramatically and the concentrations to decrease much more slowly with distance.

Stability class E produces the highest 3-hour concentration, 281 $\mu g/m^3$, and would be very likely to occur at night during any season. A plume emitted into a very stable atmosphere of class F stability apparently experiences a significant horizontal dispersion before peaking at the surface far downwind, and therefore, produces lower concentrations. It must be remembered that the wind speeds used for these cases are typical wind speeds for each stability class, and that a total range of speeds has not been tested.

All computed Base Case 3-hour SO_2 concentrations are well below the Class

II PSD allowable increment (512 $\mu g/m^3$) from 0.25 to 10.0 km. Cases 3, 9, 10 and 11, however, greatly exceed the Class I increment (25 $\mu g/m^3$) at all distances. Only Case 1 showed concentrations dropping below the Class I increment level beyond 5.2 km.

Long Term Results

Annual CDM modeling results for the Base Case and Option 2 Case smelter model are presented in Figures 38 and 39. These results include both the stack and fugitive emissions, assuming normal operating conditions. Isopleths were plotted by computer for 2 $\mu g/m^3$ (the class I annual PSD allowable SO_2 increment) and for every 5 $\mu g/m^3$ for the Base Case and for 0.5, 1 and 2 $\mu g/m^3$ for the Option 2 case.

The resulting average dispersion patterns, as expected, strongly reflect the annual wind rose. For the Base Case (Figure 28) a large area of computed concentrations between 10 and 15 $\mu g/m^3$ lies to the SSE of the smelter and a much smaller area lies to the north. Computed concentrations at all points are less than the Class II PSD allowable increment of 20 $\mu g/m^3$, but a possible factor of two error in the modeling could lead to exceedances of that level. The Class I increment, 2 $\mu g/m^3$, is estimated to be exceeded out to about 30 km to the SSE and out to about 10 km in all directions. Model accuracy certainly deteriorates with distance, but it is clear that the Class I increment would be jeopardized over a considerable area. Levels from an Option 2 smelter (Figure 39) would be much lower than these from a Base Case smelter. Concentration increments of 2 $\mu g/m^3$ are predicted out to 6 km from the source.

No seasonal meteorological summaries were available for Hibbing, but they were available for International Falls. CDM modeling results showed the

seasonal variations from the mean, computed along the four principle compass directions, to be within about ± 25% of the annual mean. A visual analysis of the monthly roses for Hibbing (Watson, 1978a) indicates that similar seasonal variations could be expected for Hibbing, also.

Smelter Upset Conditions

The above modeling results have all dealt with the smelter assuming normal operating conditions. Another important issue concerns effluent release during smelter upset conditions. Two general cases of upset conditions leading to SO_2 release are considered here:

(1) Stack upset: The first case would occur during the failure of a major piece of air pollution control equipment such as the acid plant. All the SO_2 normally treated by the control equipment is then assumed to bypass the acid plant and be released directly to the atmosphere through the stack. This SO_2 release would thus include the strong gas stream (10,031 gm/sec) as well as 90% of the weak gas stream normally collected (295 gm/sec) for a total of 10,326 gm/sec of SO_2. The normal operating conditions fugitive SO_2 release rate of 33 gm/sec would continue to occur unaltered. This type of upset condition is assumed to occur for a few hours (during which repairs would be made or smelter operations would be brought to a virtual halt). For modeling purposes, these emission rates were assumed to last for three hours.

(2) Fugitive upset: The second upset is intended to simulate a situation which might occur if a major equipment failure were to lead to the low level release of all the SO_2 normally treated by the air pollution control equipment (such as a crane accidentally breaking the duct to the acid

plant). Such a break occurrence, though highly unlikely, is conceivable and could cause the release of all the strong and weak SO_2 streams, a total of 10,359 gm/sec, as fugitive emissions. This emergency situation would certainly lead to a smelter shut-down as soon as possible. In reality, the period of release could be from a few minutes to a few hours, depending on the nature of the smelting equipment being used and the response of the smelter personnel. Purely for model purposes, such emissions were assumed to last for three hours.

Dispersion Modeling and Results

A typical worst dispersion case for the stack upset release would occur during periods of light wind with unstable conditions such as occur during sunny days. The meteorological conditions used in the modeling were chosen for the 3-hour case #3 (Table 13) which has a slightly unstable atmosphere (Class C).

Stack parameters were the same as for normal operating conditions except that the exit gas temperature was assumed to be raised to 300°C to reflect the loss of cooling which normally occurs during acid manufacturing. Three-hour ground level concentrations were computed with the TEM (for the upset stack release) and the Fugitive Model (for the normal fugitive release). The results for the TEM are presented in Figure 40. The maximum concentration is 1690 $\mu g/m^3$ at 3.8 km downwind, about seven times greater than the concentration for the Base Case Model during normal operations with the same meteorological conditions. The peak concentrations would also occur farther downwind than under normal conditions because the higher exit gas temperature yields greater plume rise.

A worst dispersion case for the fugitive upset release, on the other hand,

occurs with a stable atmosphere which prevents the plume released near ground level from dispersing rapidly downwind. The case selected for modeling was very stable case #11 of the 3-hour cases (see Table 13). This case estimates concentrations under stability class F which occurs at night during all seasons. Results of computations with the Fugitive Model are presented in Figure 41. Computed concentrations are extremely high. The level is about 76,000 $\mu g/m^3$ at 0.25 km and decreases exponentially with distance. These concentrations are much higher than those computed for the upset release; in fact, they are about 27 times greater than the concentrations for the stack release case at 3.8 km, the distance of maximum stack release concentrations.

Most of the difference between these two sets of smelter upset results is real. A plume released into very stable air near the surface is expected to cause considerably higher concentrations than is a hot plume released through a stack. Part of this difference is probably artificial, however. Gaussian models do not deal well with stable conditions, and as discussed previously, the Fugitive Model is considered to be conservative for stable atmospheres. Thus, the specific values predicted here should be viewed as order of magnitude projections only.

REFERENCES

American Meteorological Society, Committee on Atmospheric Turbulence and Dispersion. 1978. Accuracy of dispersion models. Bulletin of the American Meteorological Society. V.59. August, 1978.

Bowers, J.F. 1977. Personal communication.

Briggs, G.A. 1969. Plume rise. AEC Critical Review Series (NTIS No. TID-25075), Atomic Energy Commission, Division of Technical Information. Oak Ridge, Tennessee.

Brubaker, K.L., P. Brown, and R.R. Cirillo. 1977. Addendum to user's guide for climatological dispersion model. Publication No. EPA-450/3-77-015, USEPA, Research Triangle Park, North Carolina.

Busse, A.D., and J.R. Zimmerman. 1973. User's guide to the Climatological Dispersion Model. Publication No. EPA-RA-73-024. USEPA, Research Triangle Park, North Carolina.

Christiansen, J.H. 1976. User's guide to the Texas Episodic Model. Texas Air Control Board.

Cramer, H.E., H.V. Geary, and J.F. Bowers. 1975. Diffusion-model calculations of long-term and short-term ground level SO_2 concentrations in Allegheny County, Pennsylvania. Publication No. EPA-903/9-75-18 (NTIS No. 245262/AS) USEPA.

Garland, J.A. 1977. Dry and wet removal of sulfur from the atmosphere. Presented at the International Symposium on Sulfur in the Atmosphere, September 7-14, 1977. Dubrovnik, Yugoslavia.

Gifford, F.A. 1961. Uses of routine meteorological observations for estimating atmospheric dispersion. Nuclear Safety. V.2, 4.

Holzworth, G.C. 1972. Mixing heights, wind speeds, and potential for urban air pollution throughout the contiguous United States. Publication AP-101, USEPA, Research Triangel Park, North Carolina.

Pasquill, F. 1961. The estimation of the dispersion of windborne material. Meteorological Magazine. V.90, 1063.

Singer, I.A. 1961. Journal of the Air Pollution Control Association. V. 11.

Turner, D.B. 1970. Workbook of atmospheric dispersion estimates (revised). U.S. Dept. of Health, Education, and Welfare. Public Health Service Publication No. 995-AP-26.

USEPA. 1978. Guidelines on air quality models. Publication No. EPA-450/2-78-027 (DAQPS No. 1.2-080). USEPA, Research Triangle Park, North Carolina.

Watson, B.F. 1978a. Personal communication.

Watson, B.F. 1978b. The climate of the Copper-Nickel Study Region of northeastern Minnesota. Part A: the long-term climatological record. Regional Copper-Nickel Study.

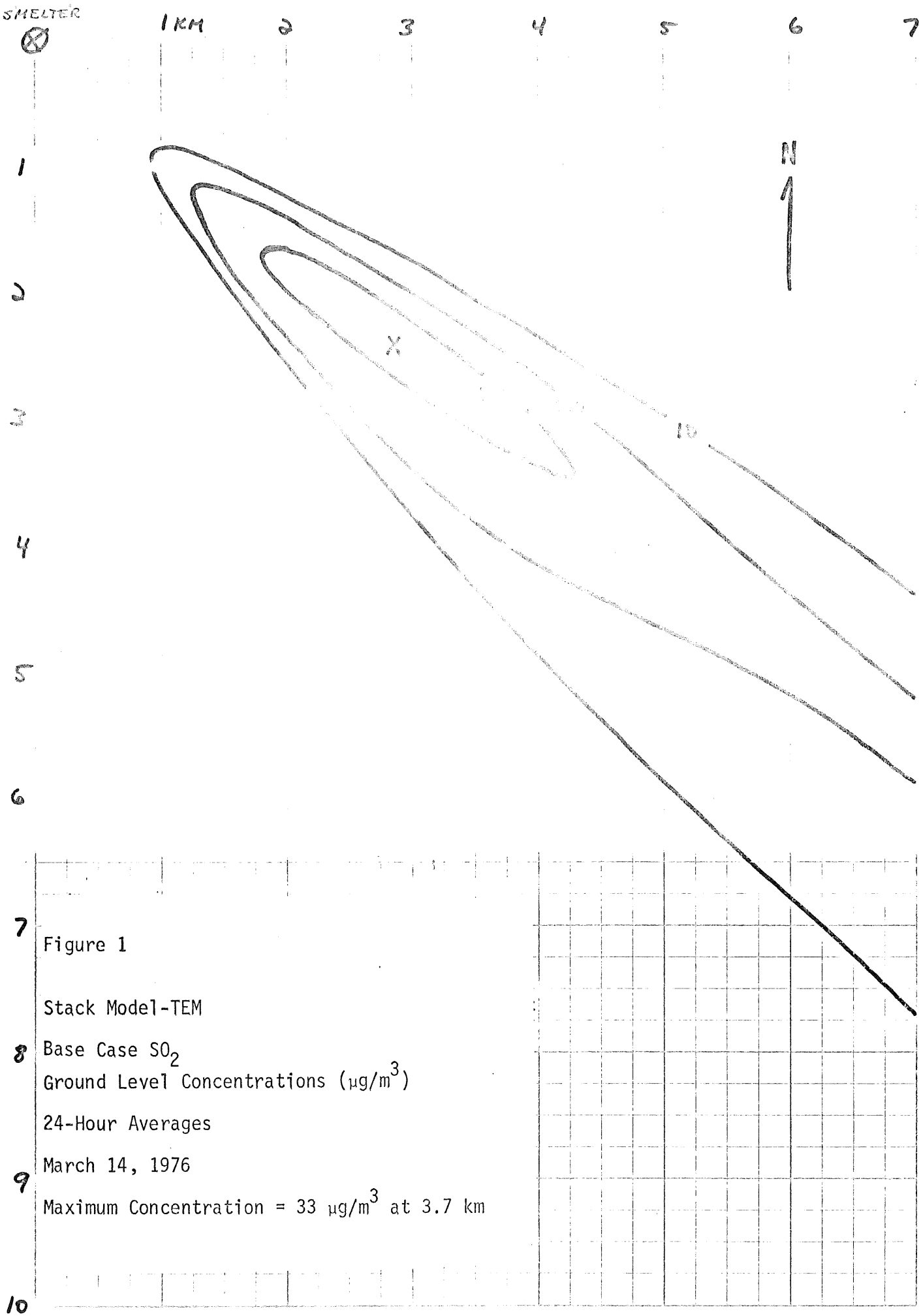

Figure 1

Stack Model-TEM

Base Case SO_2

Ground Level Concentrations ($\mu g/m^3$)

24-Hour Averages

March 14, 1976

Maximum Concentration = 33 $\mu g/m^3$ at 3.7 km

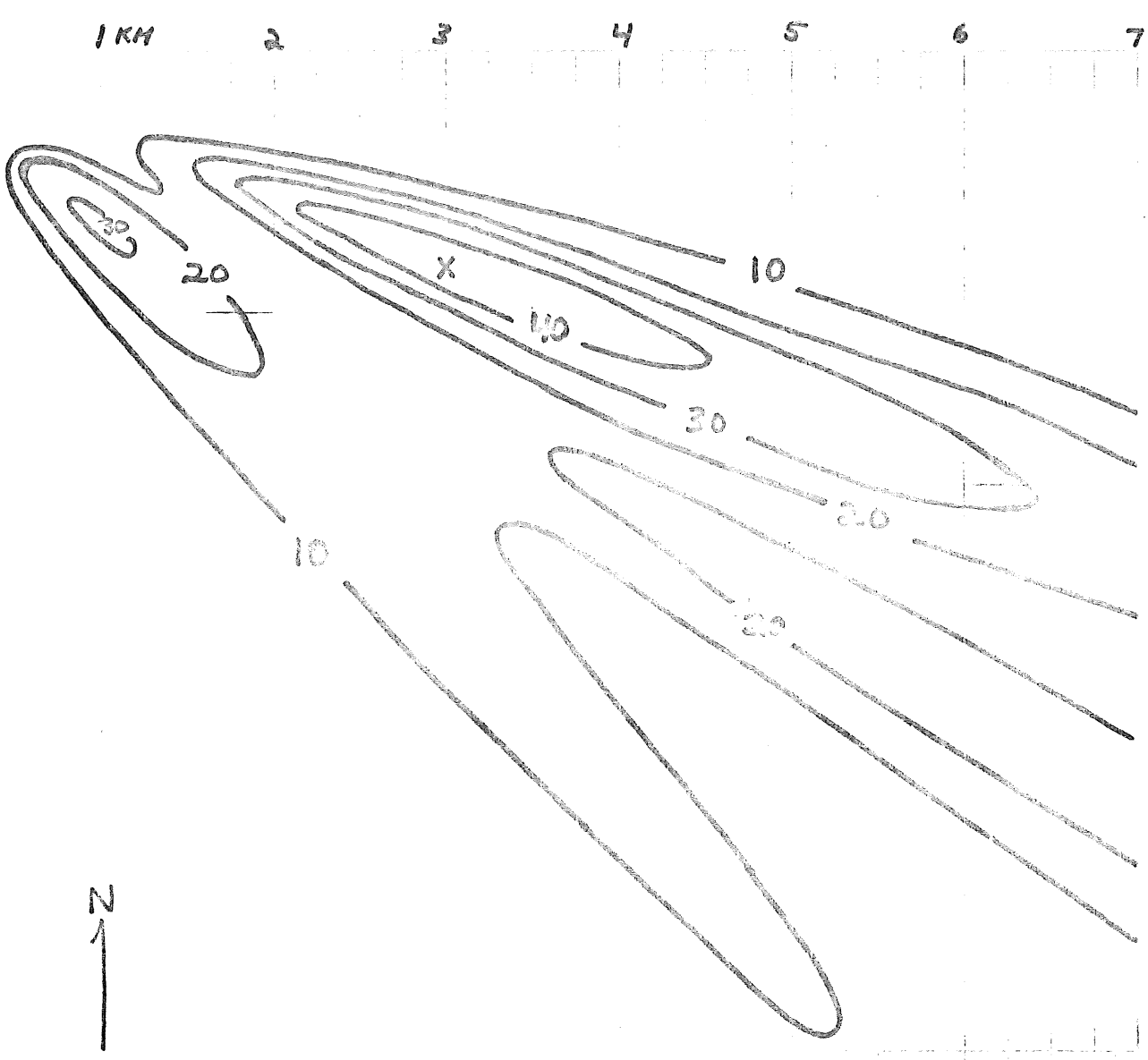

Figure 2

Stack Model-TEM

Base Case SO_2

Ground Level Concentrations ($\mu g/m^3$)

24-Hour Averages

July 23, 1976

Maximum Concentration = 46 $\mu g/m^3$ at 3.25 km

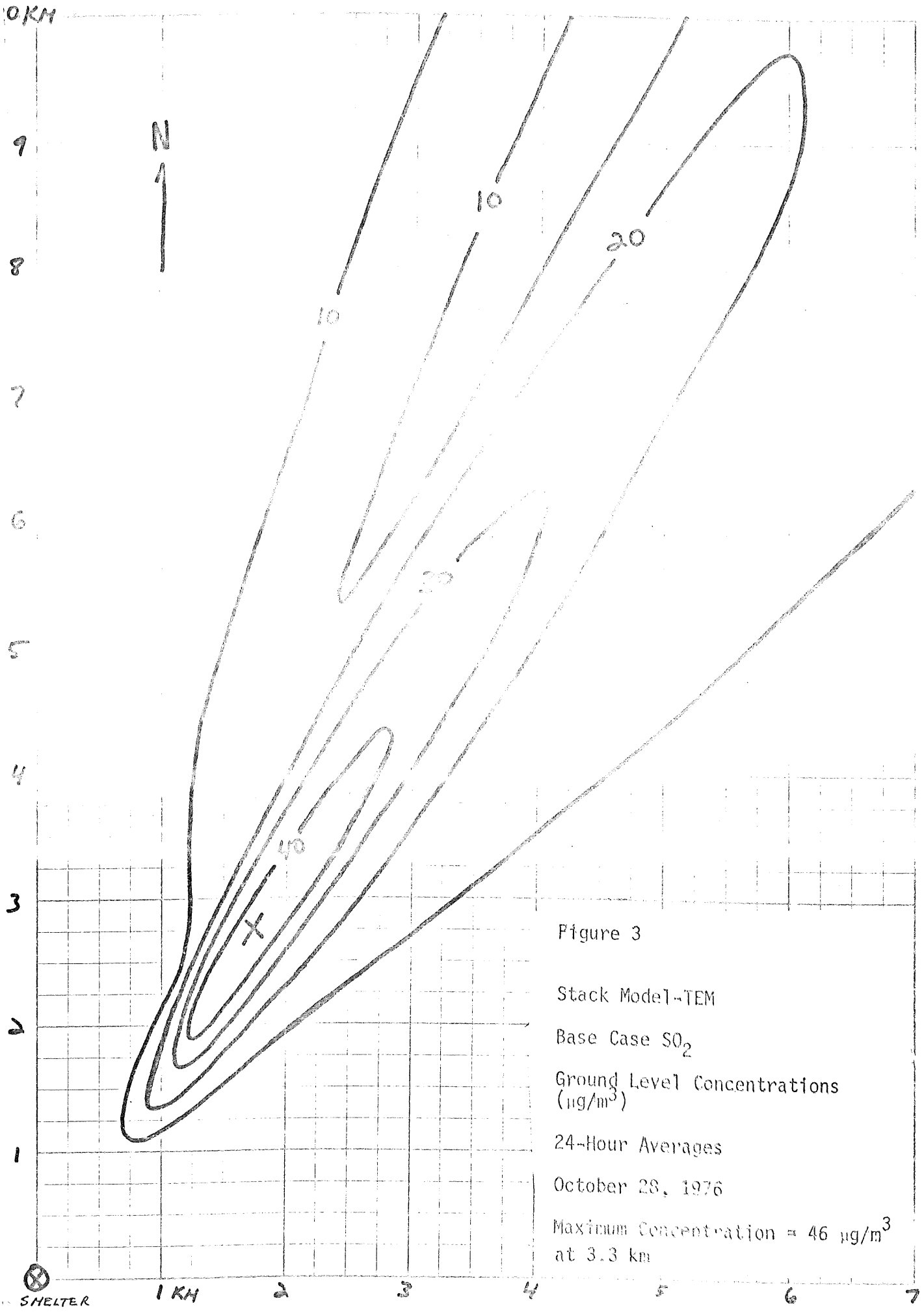

Figure 3

Stack Model-TEM

Base Case SO_2

Ground Level Concentrations ($\mu g/m^3$)

24-Hour Averages

October 28, 1976

Maximum Concentration = 46 $\mu g/m^3$ at 3.3 km

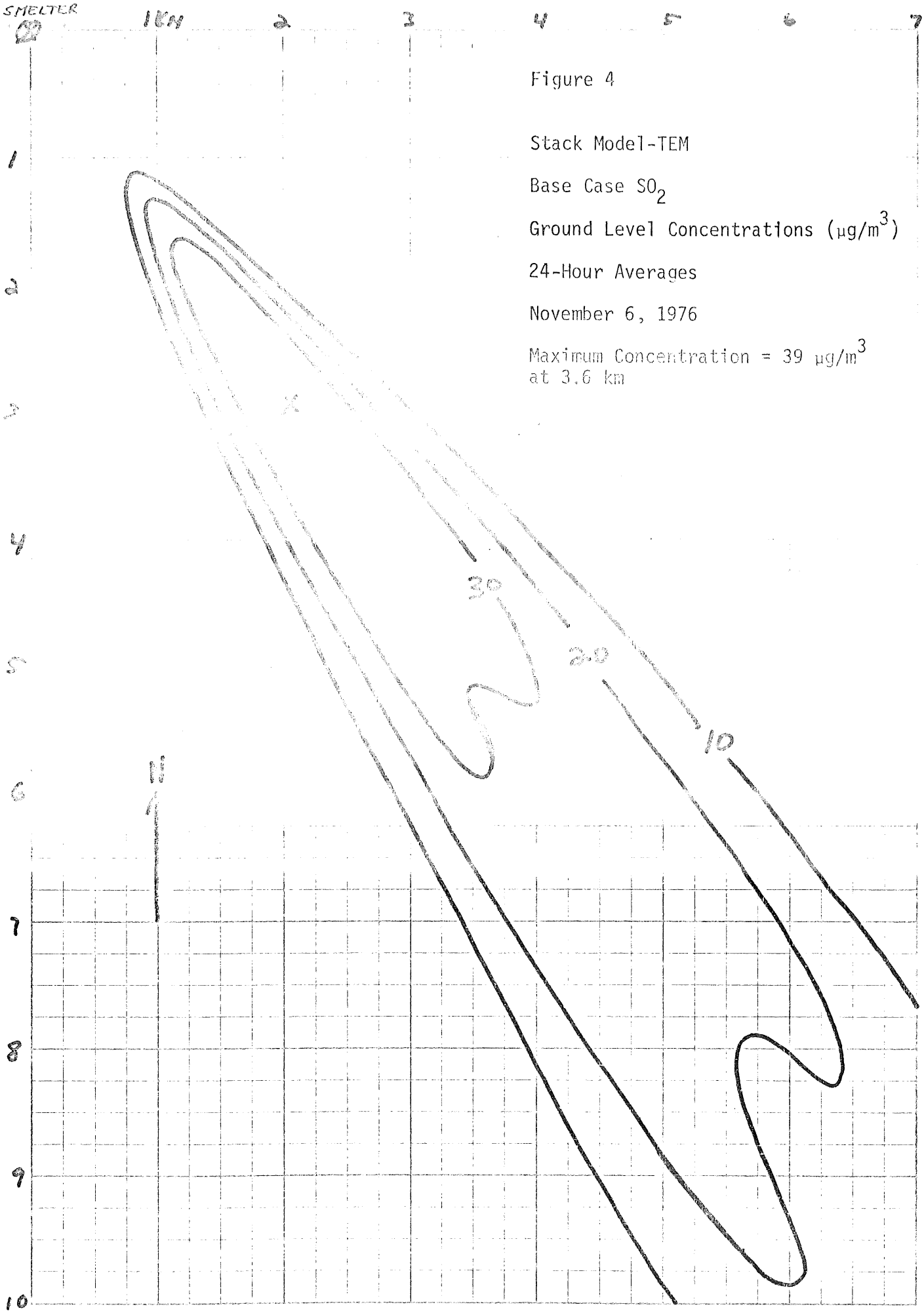

Figure 4

Stack Model-TEM

Base Case SO_2

Ground Level Concentrations ($\mu g/m^3$)

24-Hour Averages

November 6, 1976

Maximum Concentration = 39 $\mu g/m^3$
at 3.6 km

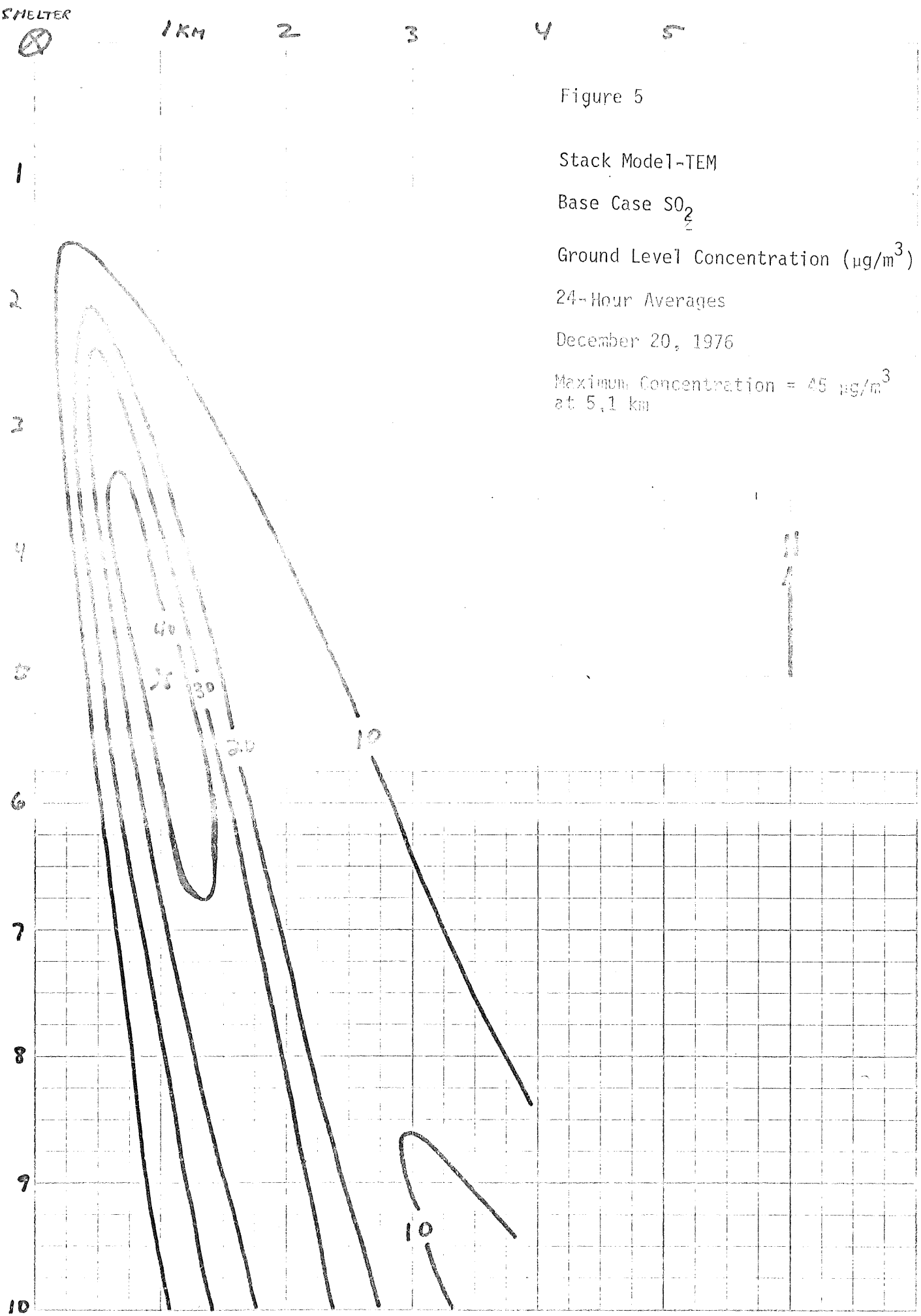

Figure 5

Stack Model-TEM

Base Case SO_2

Ground Level Concentration ($\mu g/m^3$)

24-Hour Averages

December 20, 1976

Maximum Concentration = 45 $\mu g/m^3$ at 5.1 km

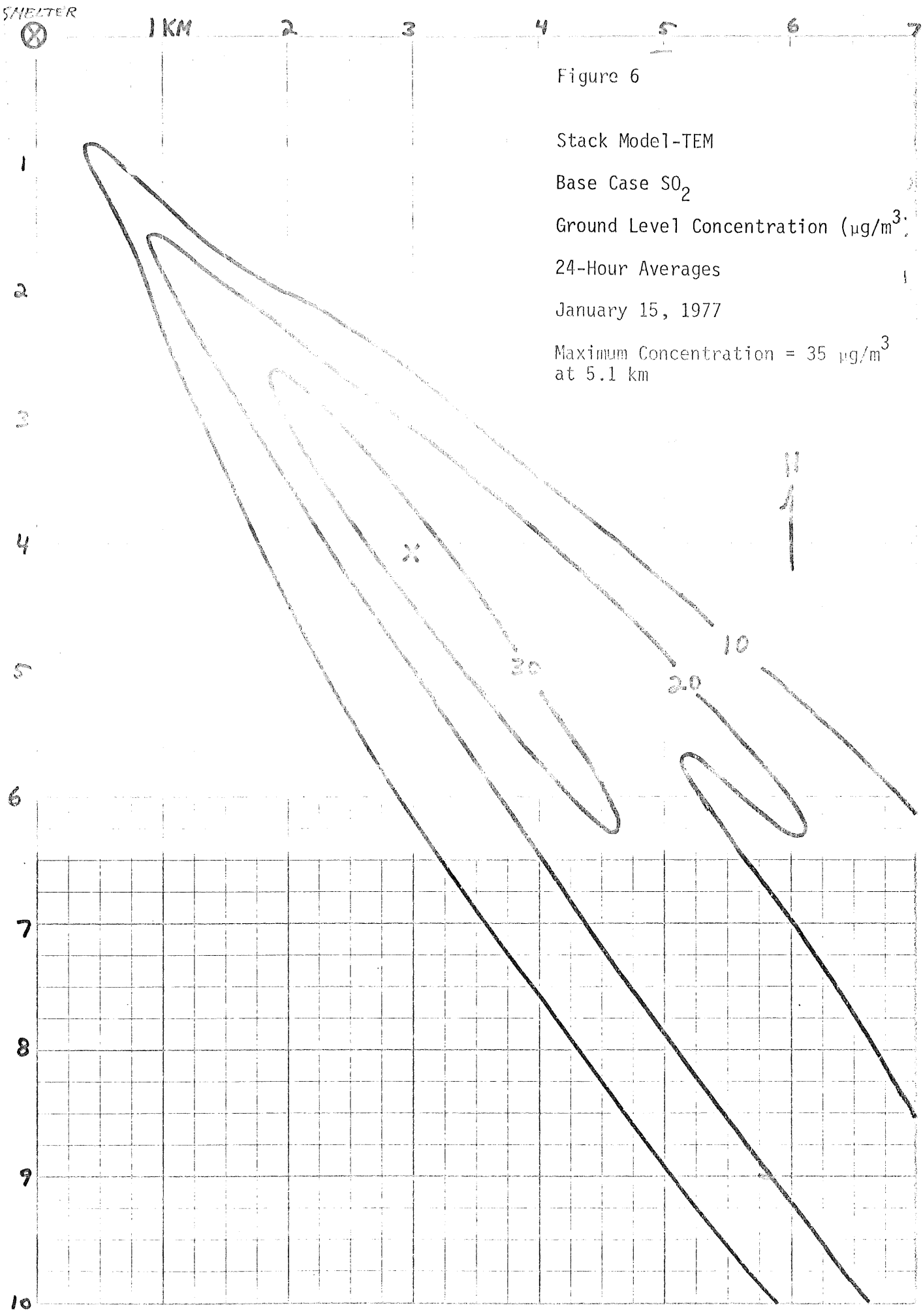

Figure 6

Stack Model-TEM

Base Case SO_2

Ground Level Concentration ($\mu g/m^3$)

24-Hour Averages

January 15, 1977

Maximum Concentration = 35 $\mu g/m^3$ at 5.1 km

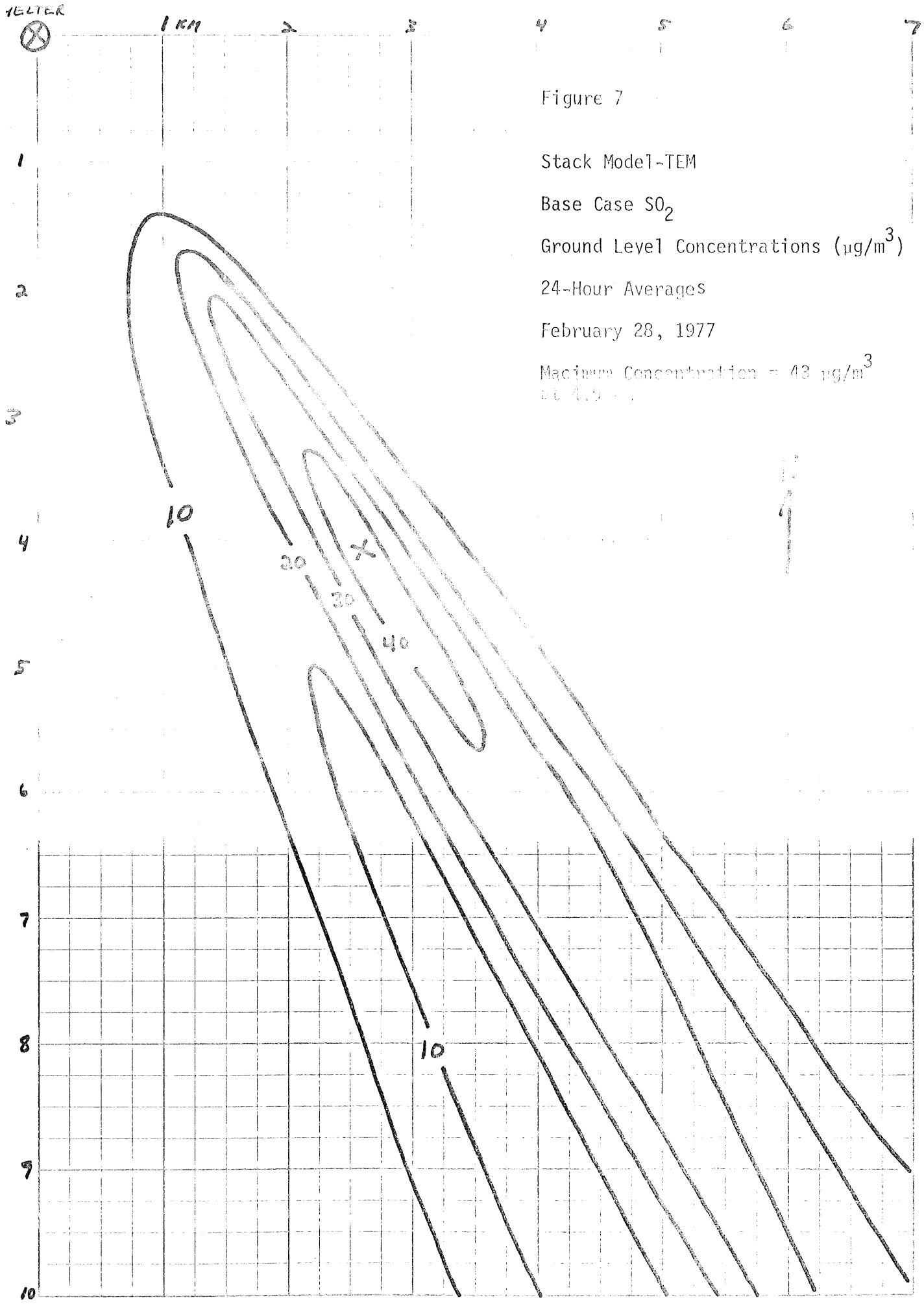

Figure 7

Stack Model-TEM

Base Case SO_2

Ground Level Concentrations ($\mu g/m^3$)

24-Hour Averages

February 28, 1977

Maximum Concentration = 43 $\mu g/m^3$
at (3,5)

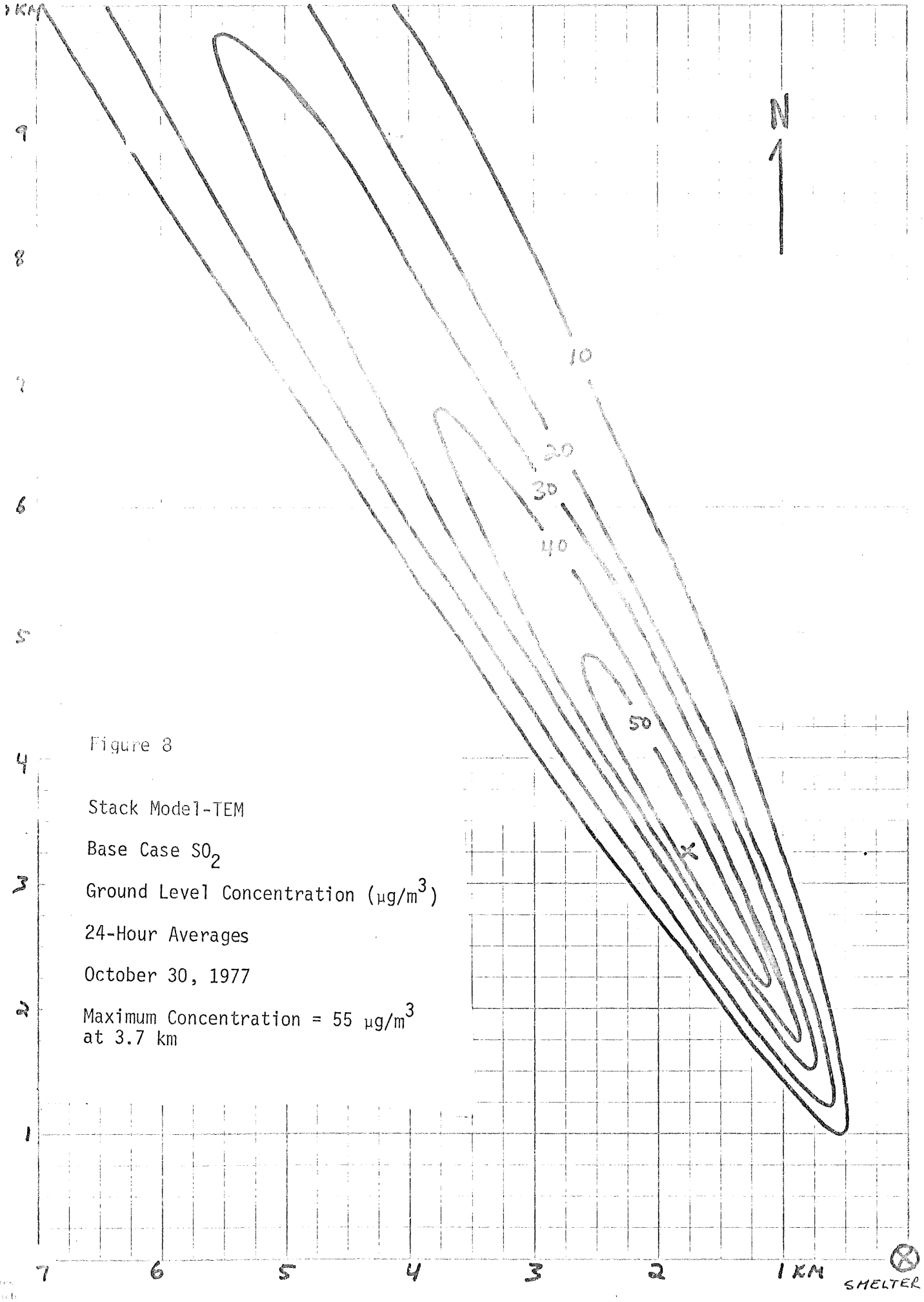

Figure 8

Stack Model-TEM

Base Case SO_2

Ground Level Concentration ($\mu g/m^3$)

24-Hour Averages

October 30, 1977

Maximum Concentration = 55 $\mu g/m^3$
at 3.7 km

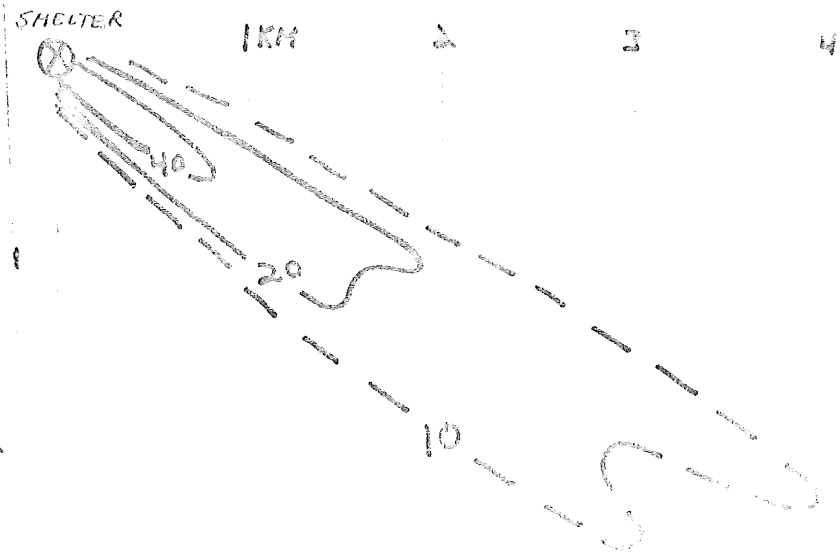

Figure 9

Fugitive SO_2 ($\mu g/m^3$)

Base Case

24-hour Averages

March 14, 1976

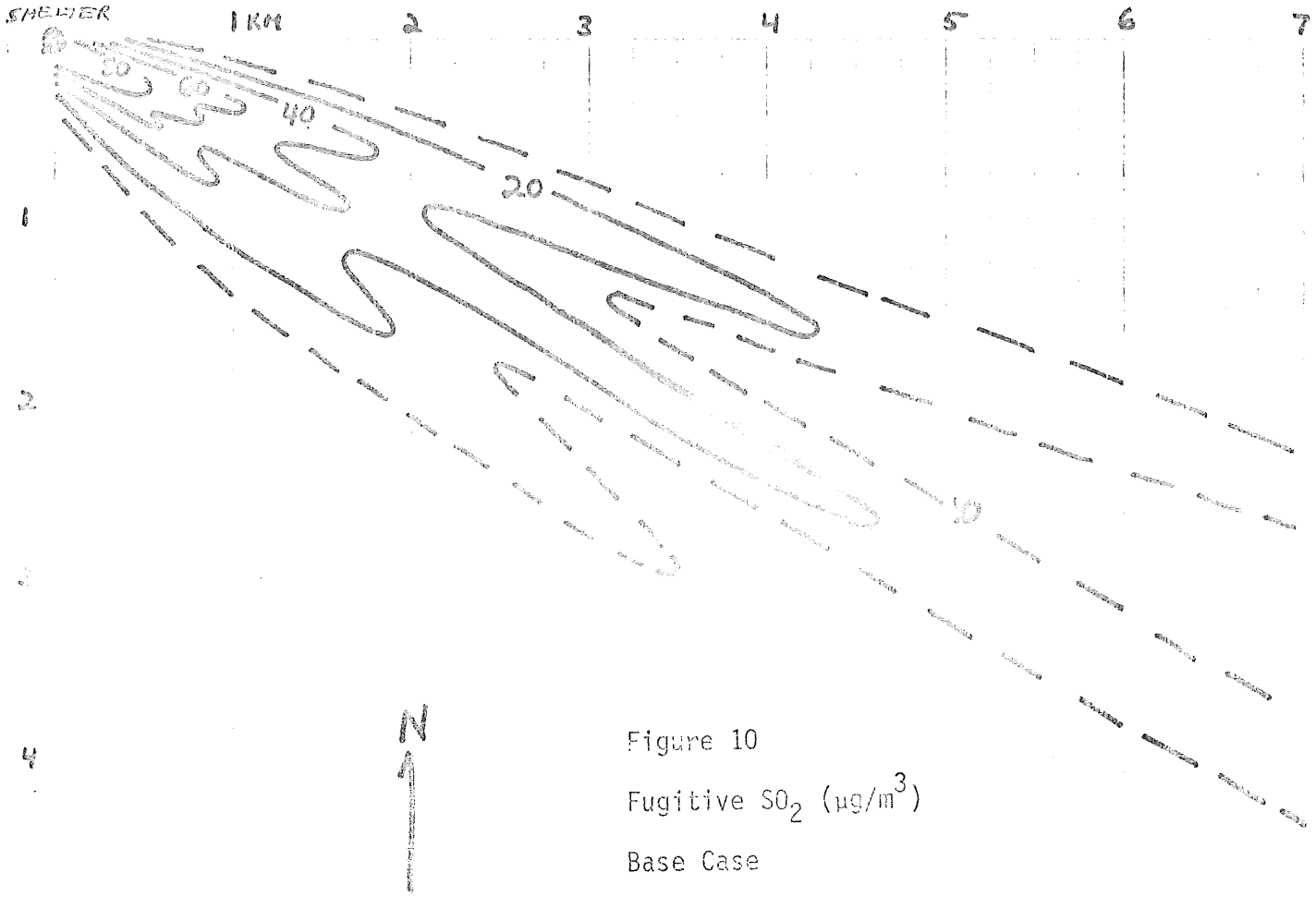

Figure 10

Fugitive SO_2 ($\mu g/m^3$)

Base Case

24-hour Averages

July 23, 1976

Figure 11

Fugitive SO_2 ($\mu g/m^3$)

Base Case

24-hour Averages

October 28, 1976

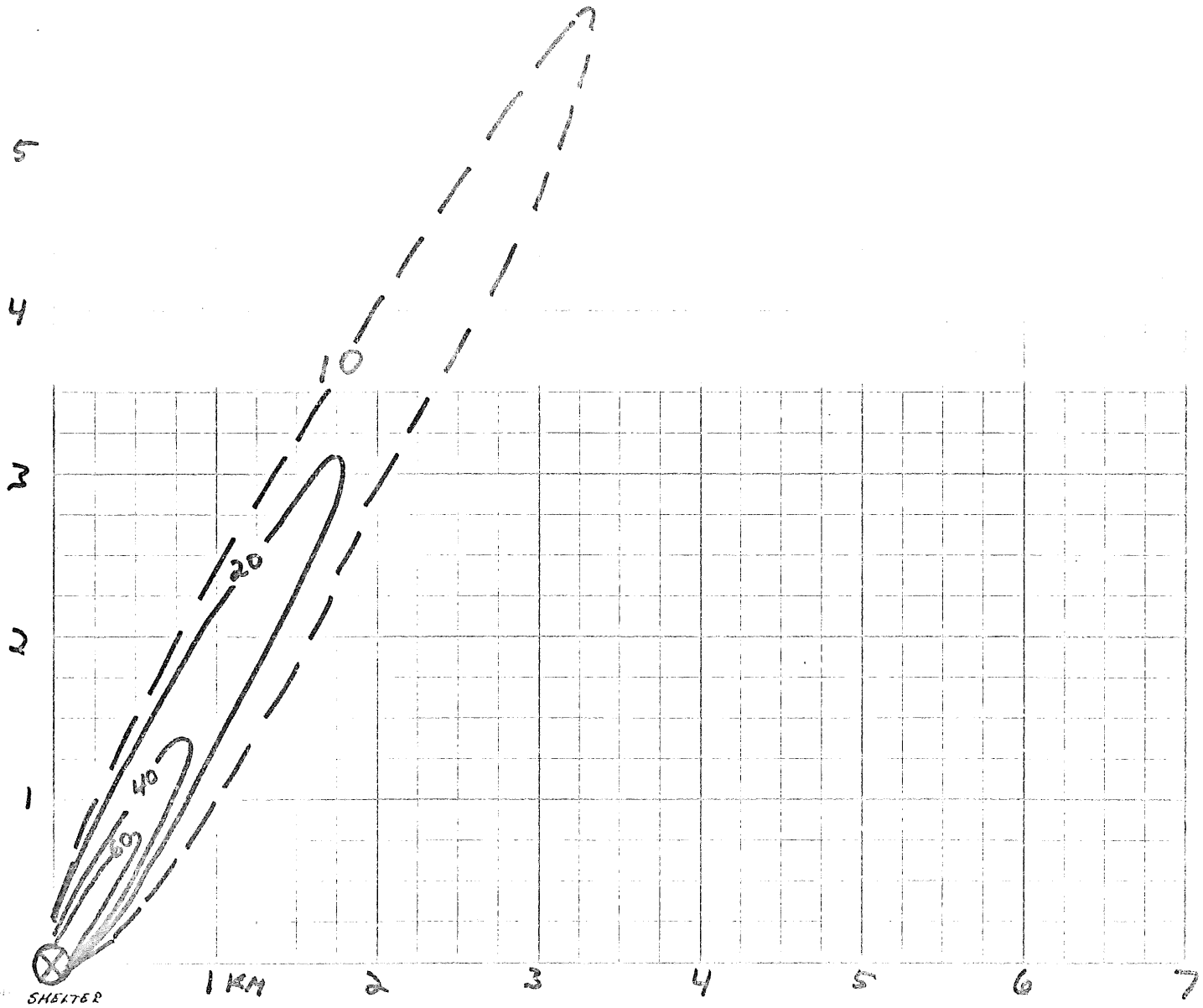

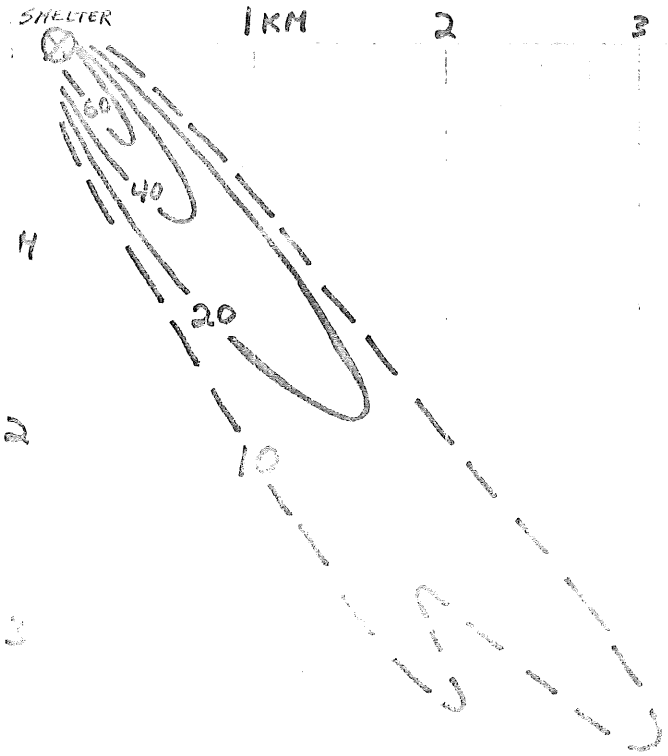

Figure 12

Fugitive SO_2 ($\mu g/m^3$)

Base Case

24-hour Averages

November 6, 1976

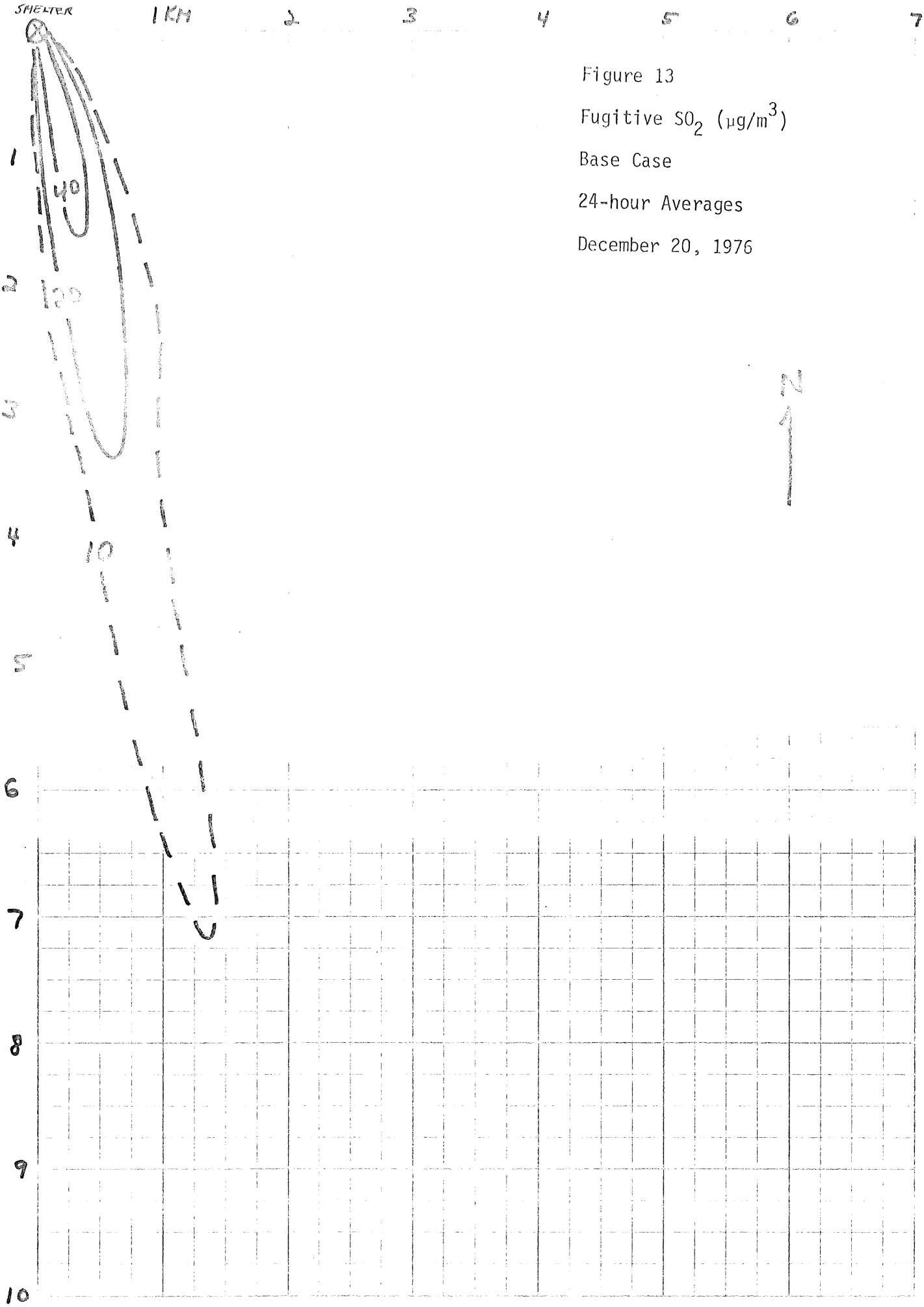

Figure 13

Fugitive SO_2 ($\mu g/m^3$)

Base Case

24-hour Averages

December 20, 1976

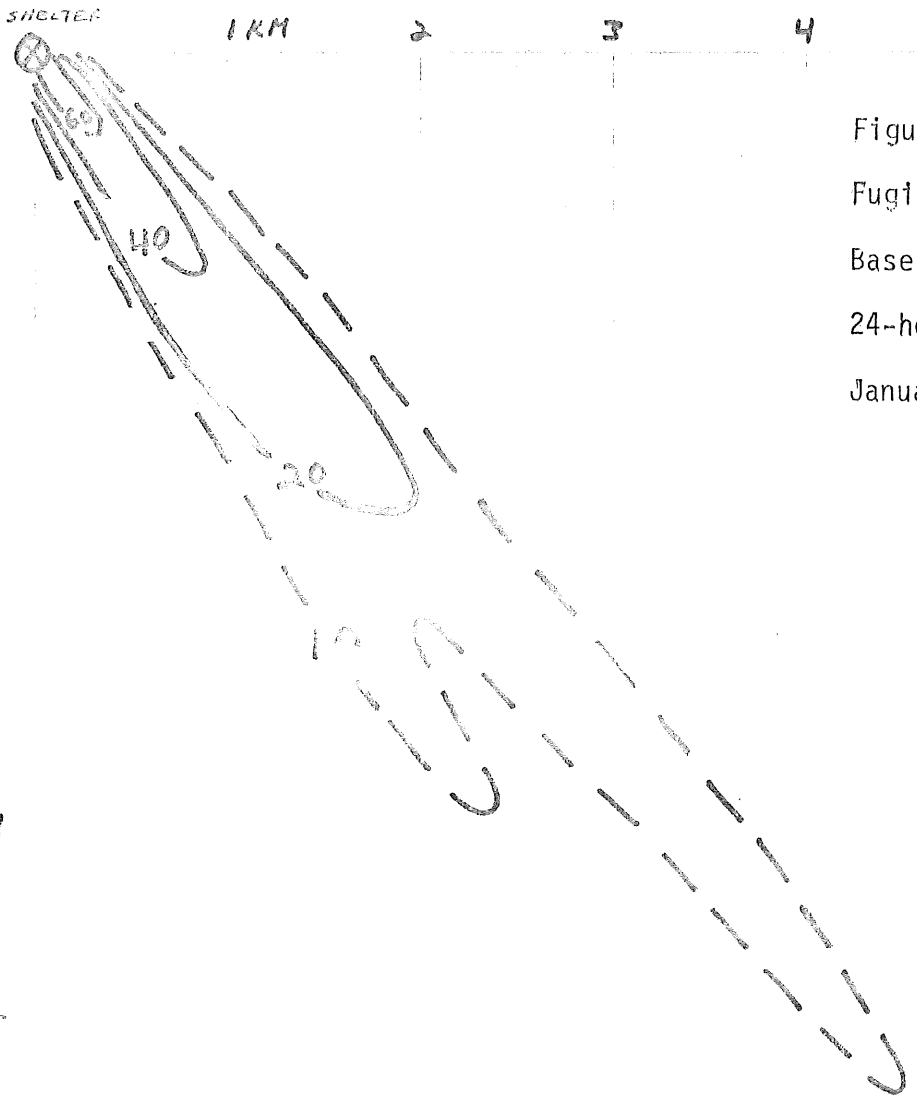

Figure 14

Fugitive SO_2 ($\mu g/m^3$)

Base Case

24-hour Averages

January 15, 1977

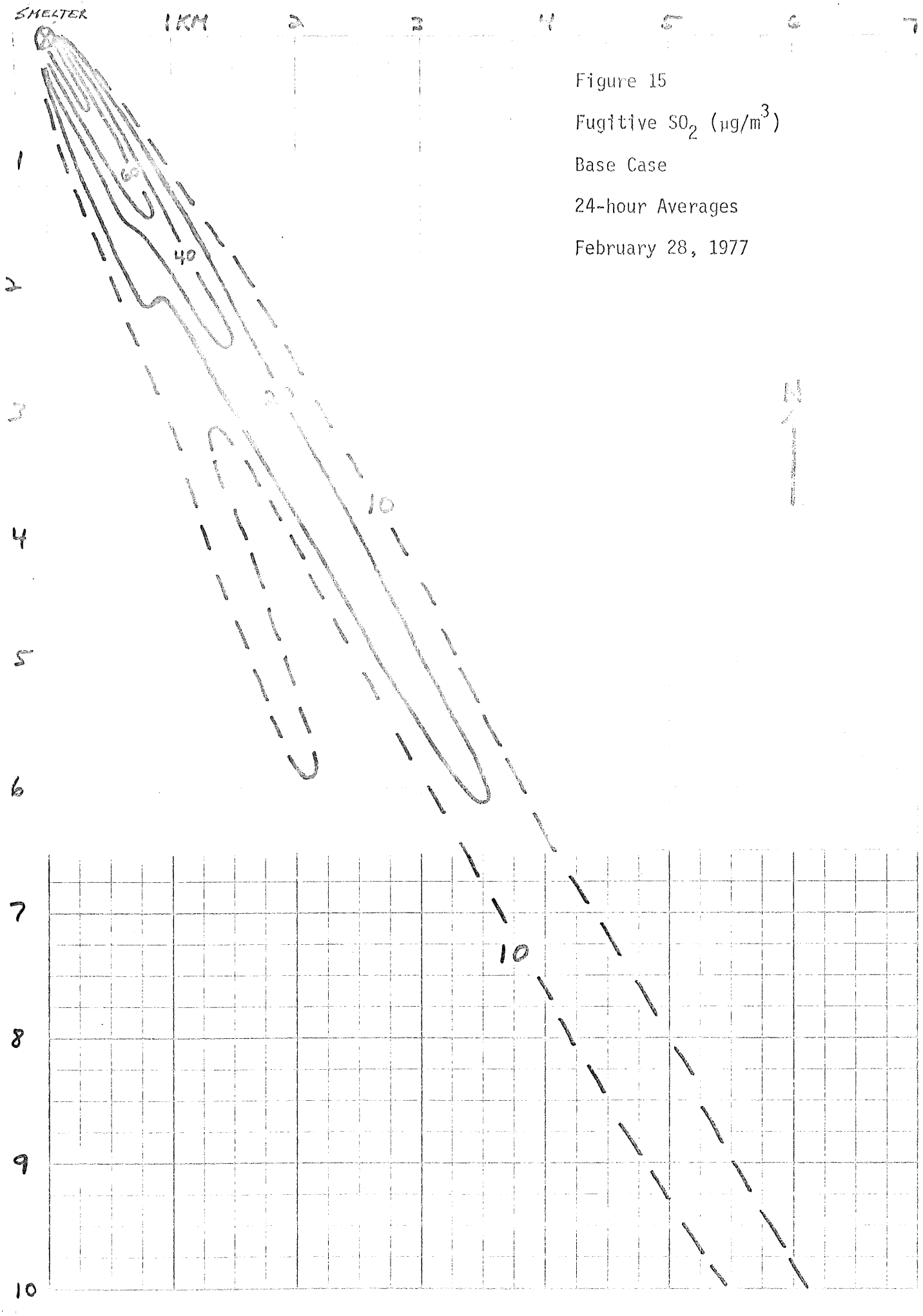

Figure 15

Fugitive SO_2 ($\mu g/m^3$)

Base Case

24-hour Averages

February 28, 1977

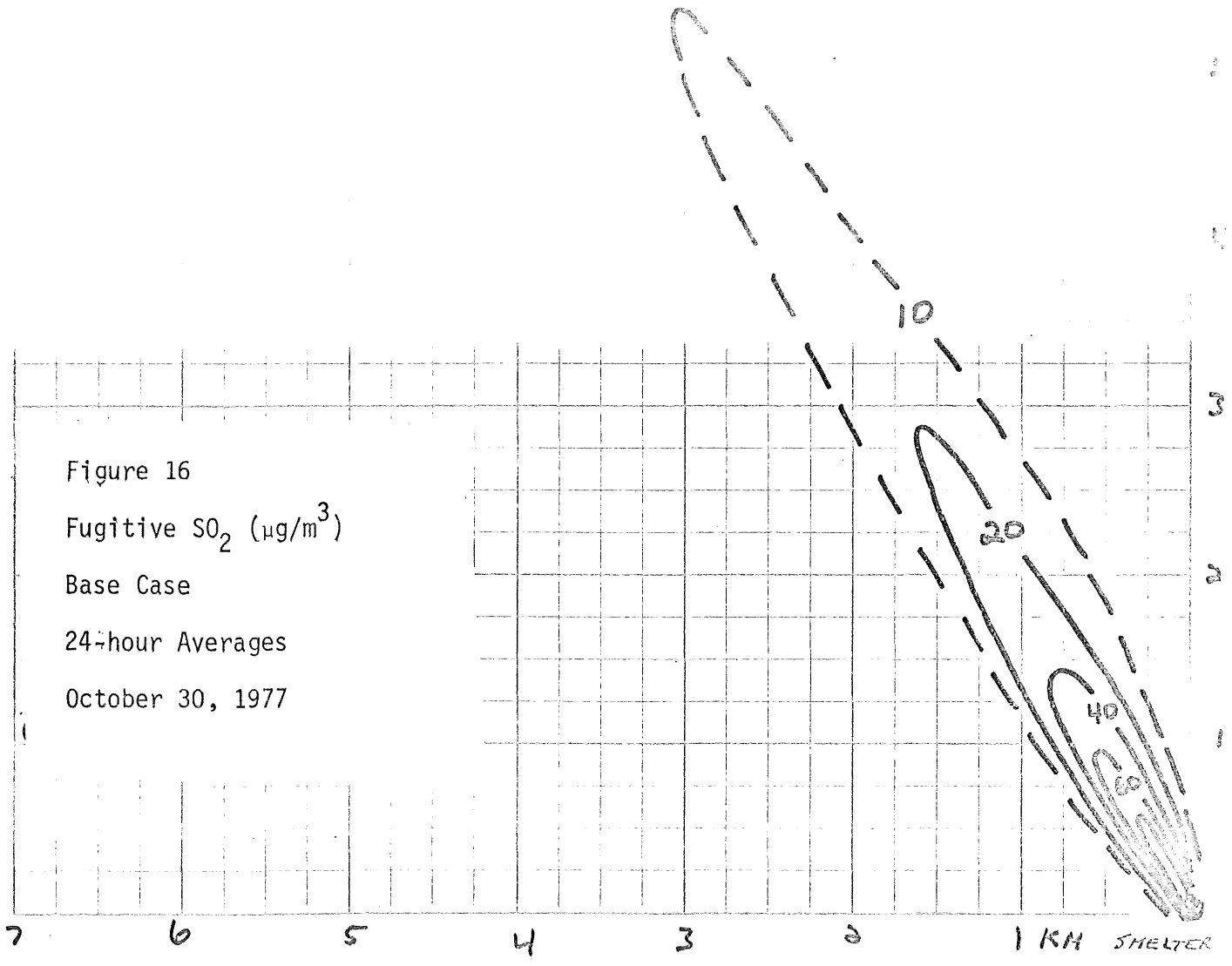

Figure 16

Fugitive SO_2 ($\mu g/m^3$)

Base Case

24-hour Averages

October 30, 1977

Figure 17

Base Case

TEST DATE March 14, 1976

Maximum 24-hour SO_2 ($\mu g/m^3$)

Ground Level Concentrations

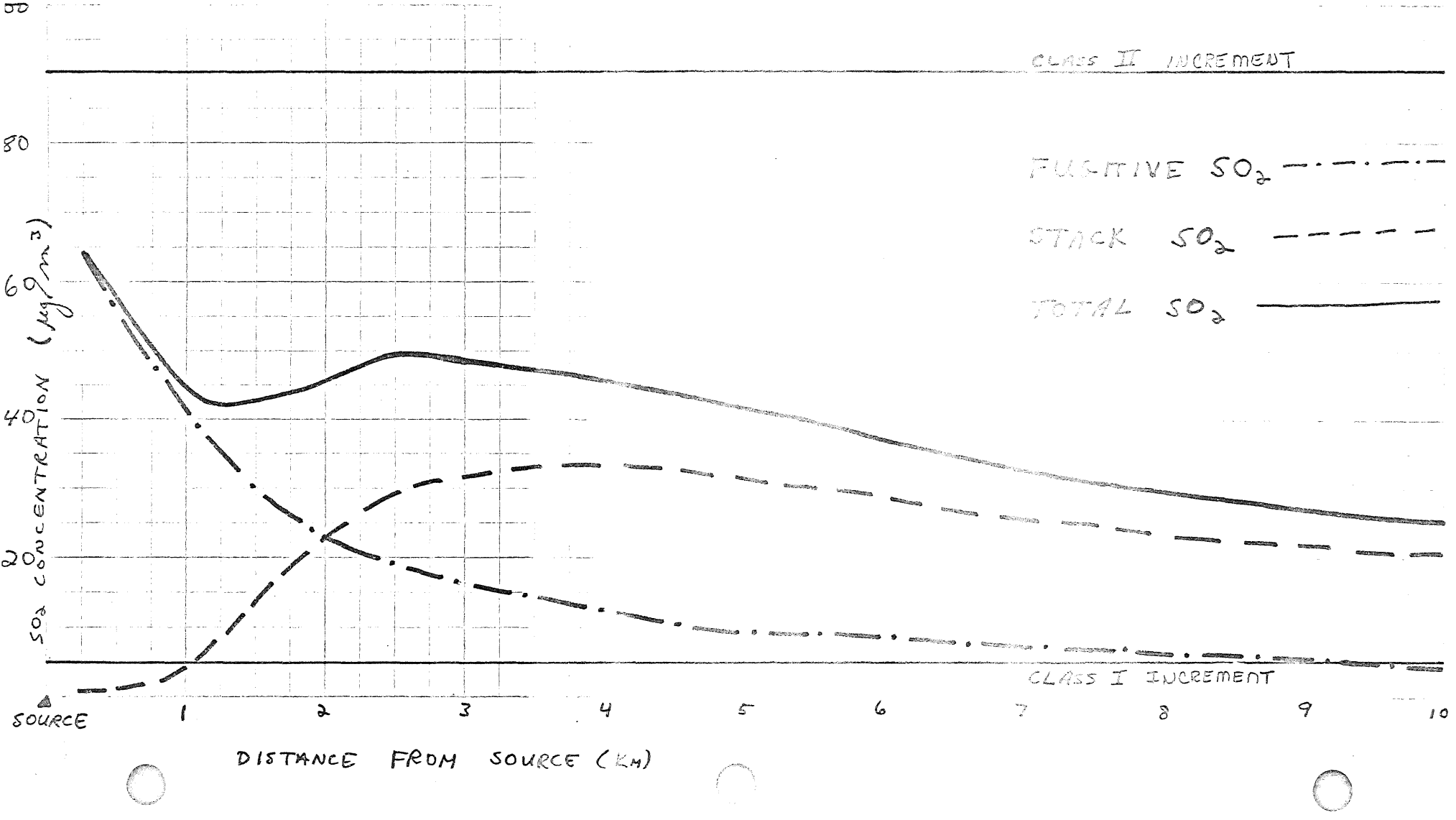

Figure 18

Base Case

TEST DATE July 23, 1976

Maximum 24-hour SO_2 ($\mu g/m^3$)

Ground Level Concentrations

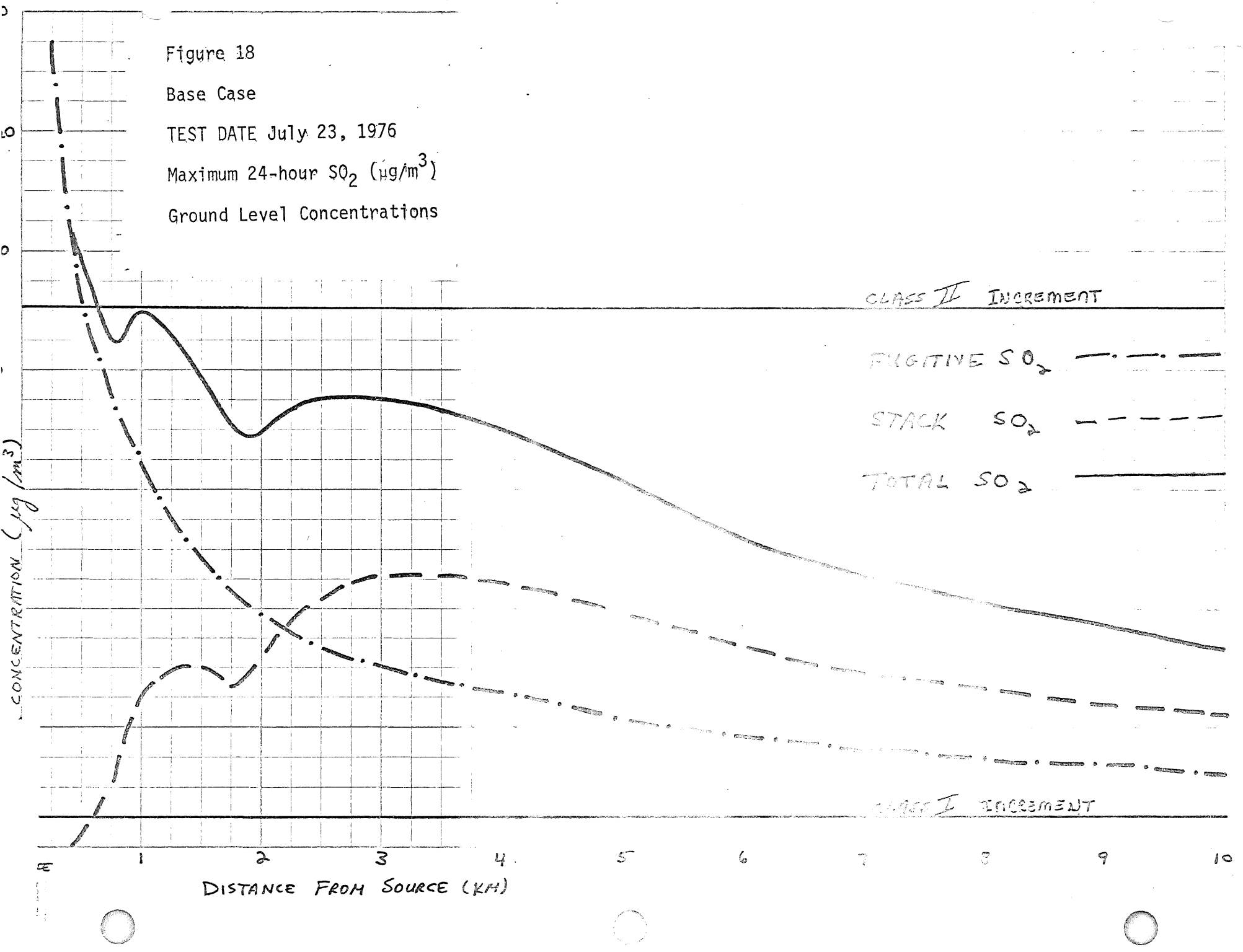

Figure 19

Base Case

TEST DATE October 28, 1976

Maximum 24-hour SO_2 ($\mu g/m^3$)

Ground Level Concentrations

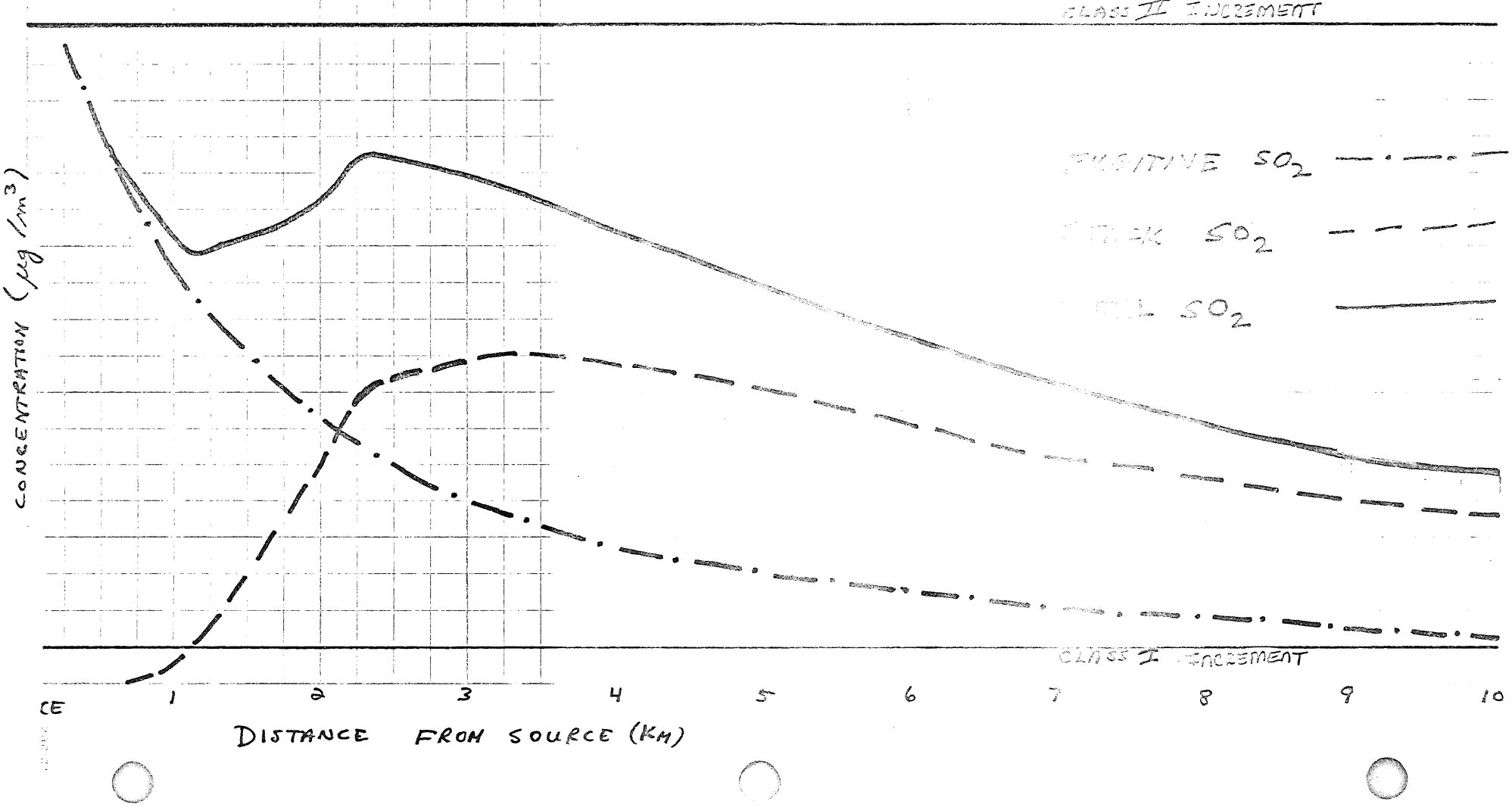

Figure 20

Base Case

TEST DATE November 6, 1976

Maximum 24-hour SO_2 ($\mu g/m^3$)

Ground Level Concentrations

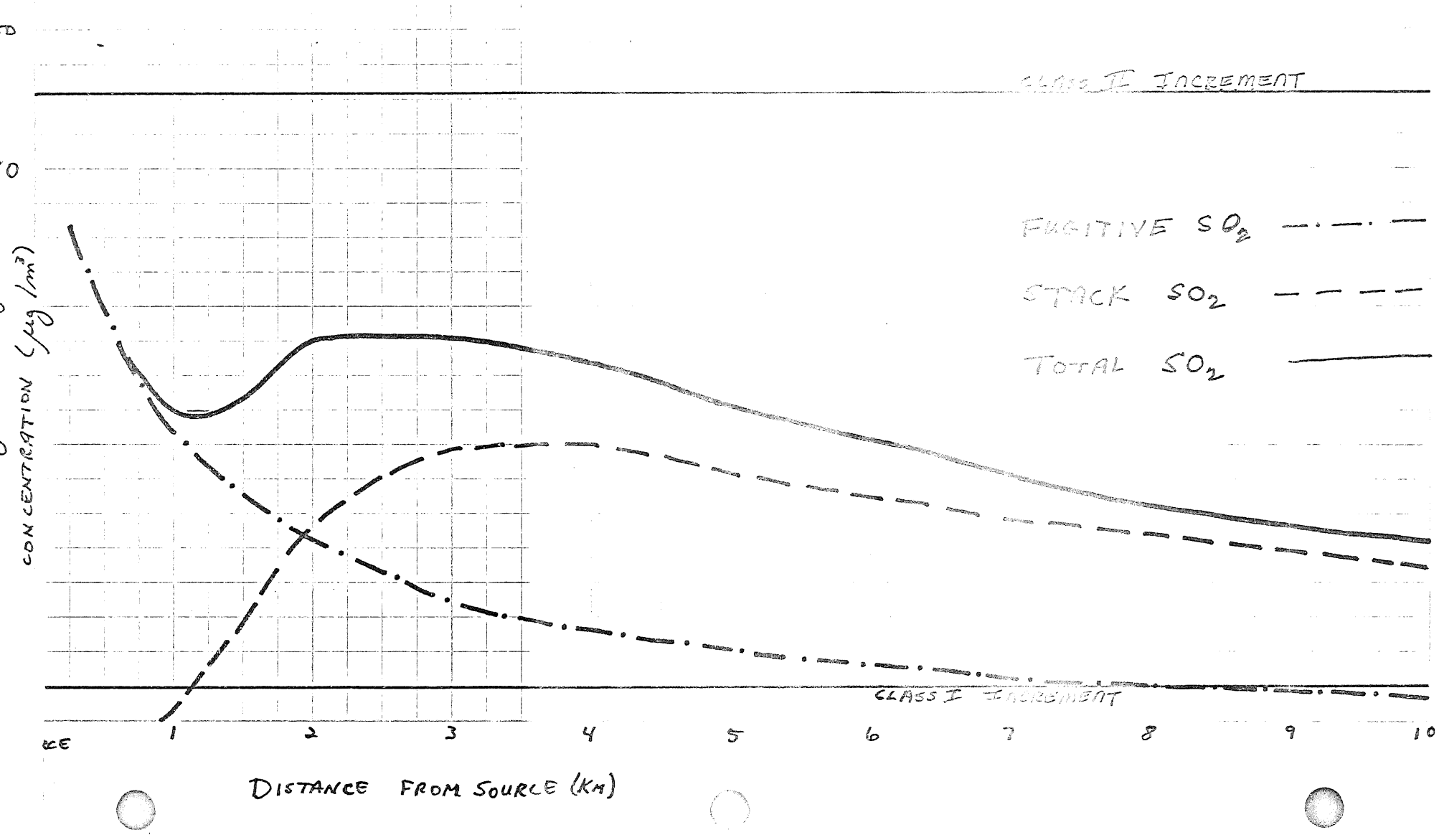

Figure 21

Base Case

TEST DATE December 20, 1976

Maximum 24-hour SO_2 ($\mu g/m^3$)

Ground Level concentrations

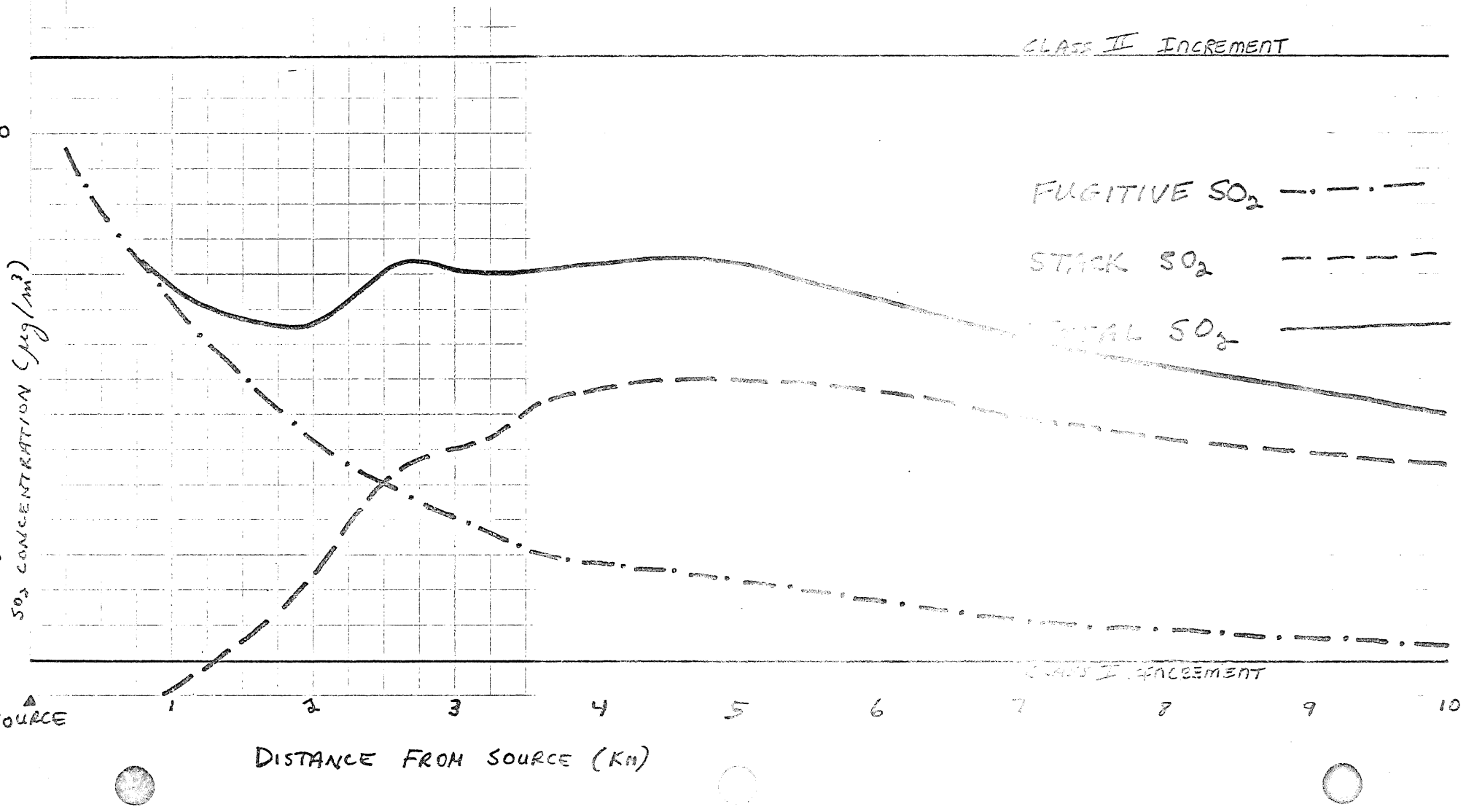

Figure 22

Base Case

TEST DATE January 15, 1977

Maximum 24-hour SO_2 ($\mu g/m^3$)

Ground Level Concentrations

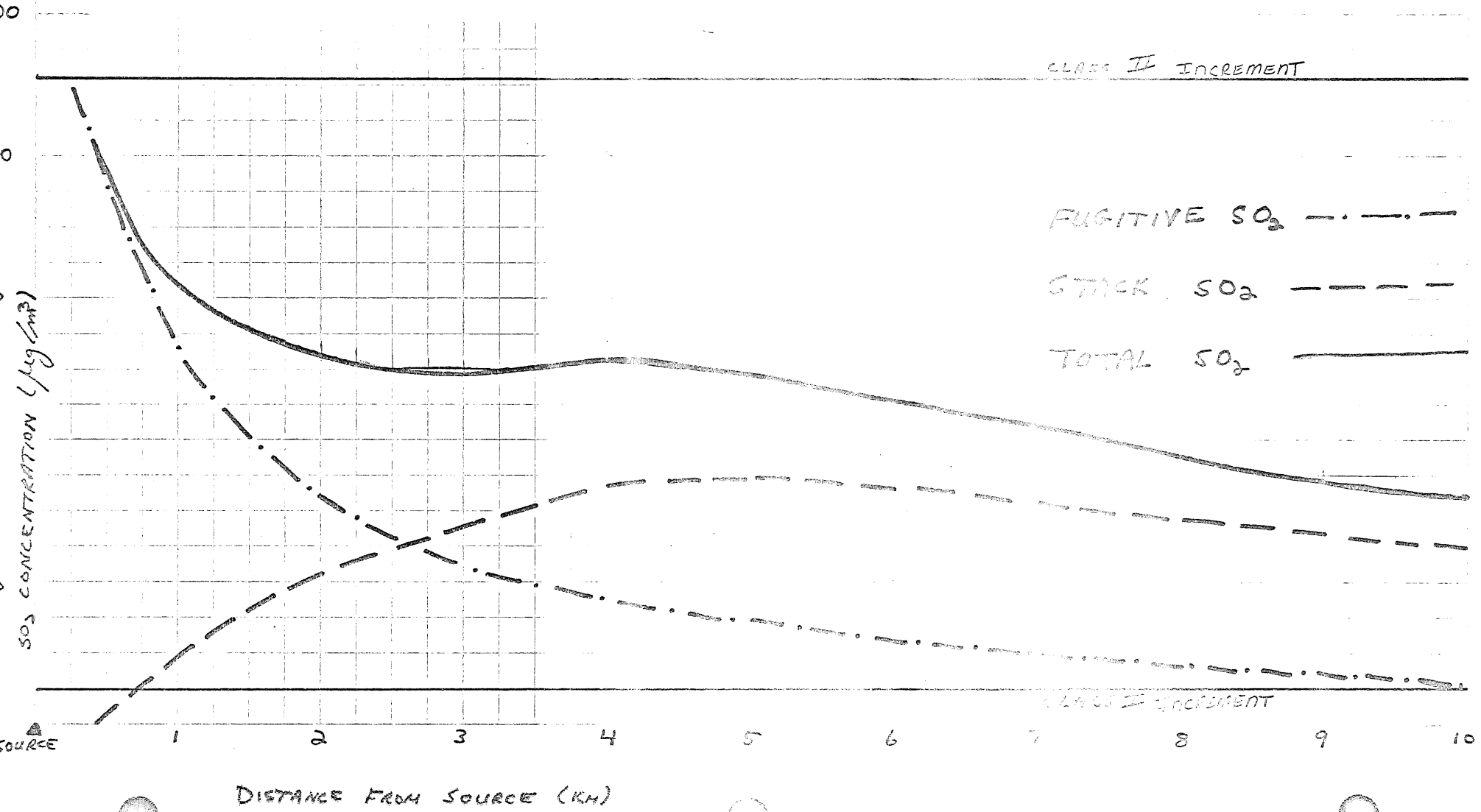

Figure 23

Base Case

TEST DATE February 28, 1977

Maximum 24-hour SO_2 ($\mu g/m^3$)

Ground Level Concentrations

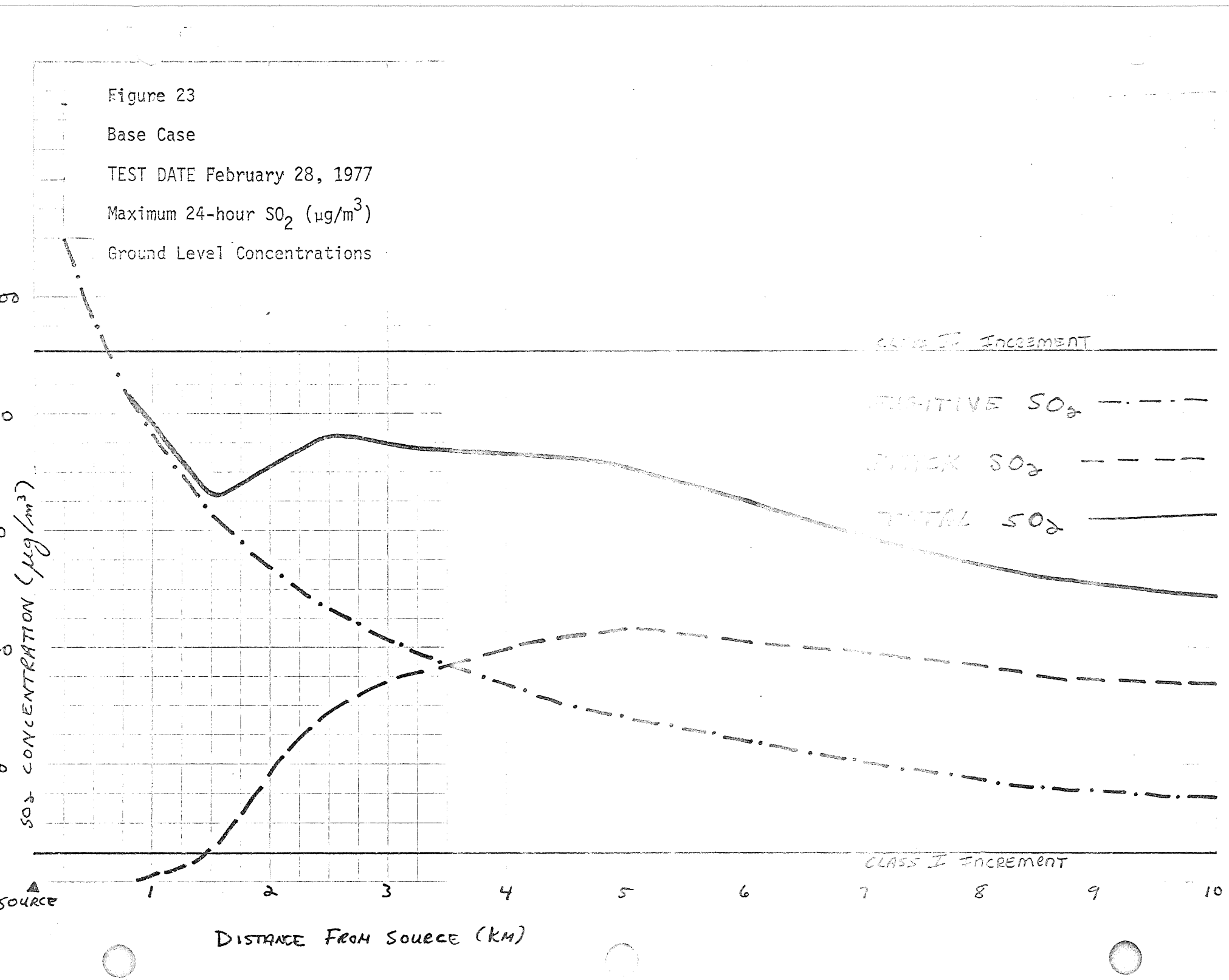

Figure 24

Base Case

TEST DATE October 30, 1977

Maximum 24-hour SO_2 ($\mu g/m^3$)

Ground Level Concentrations

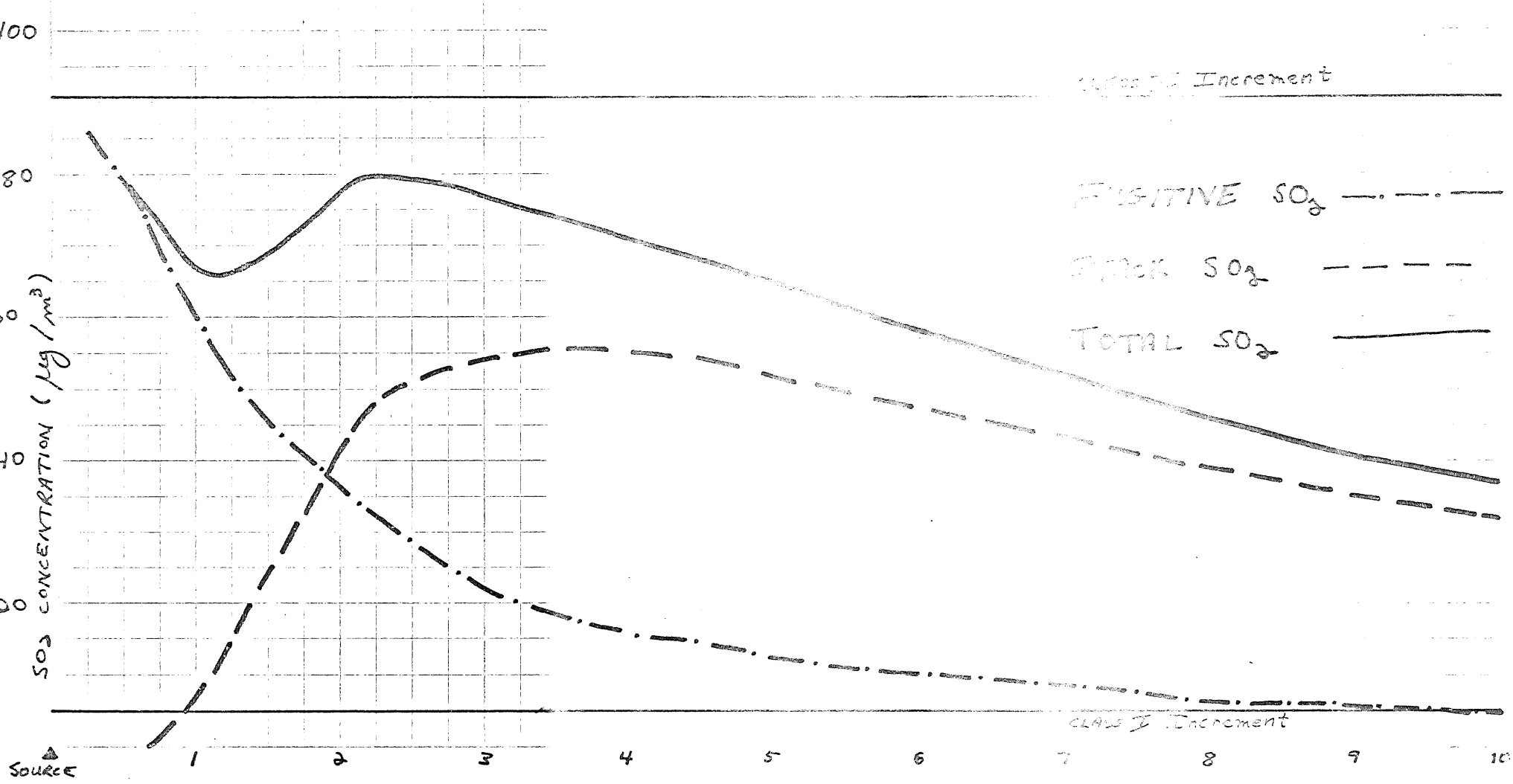

Figure 25

High Fugitive Basic Model

July 23, 1976

24-hour SO_2 ($\mu g/m^3$)

Ground Level Concentrations

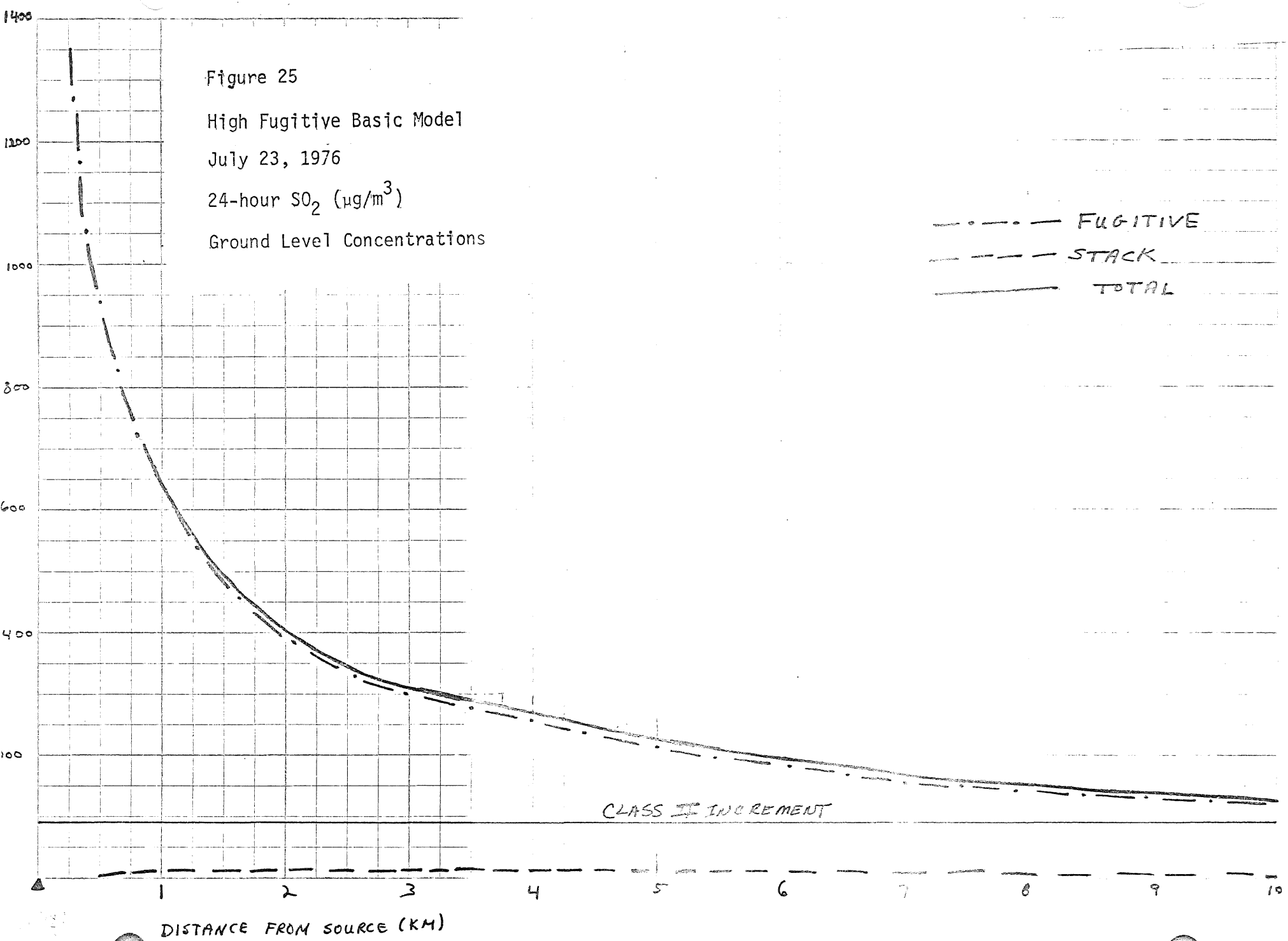

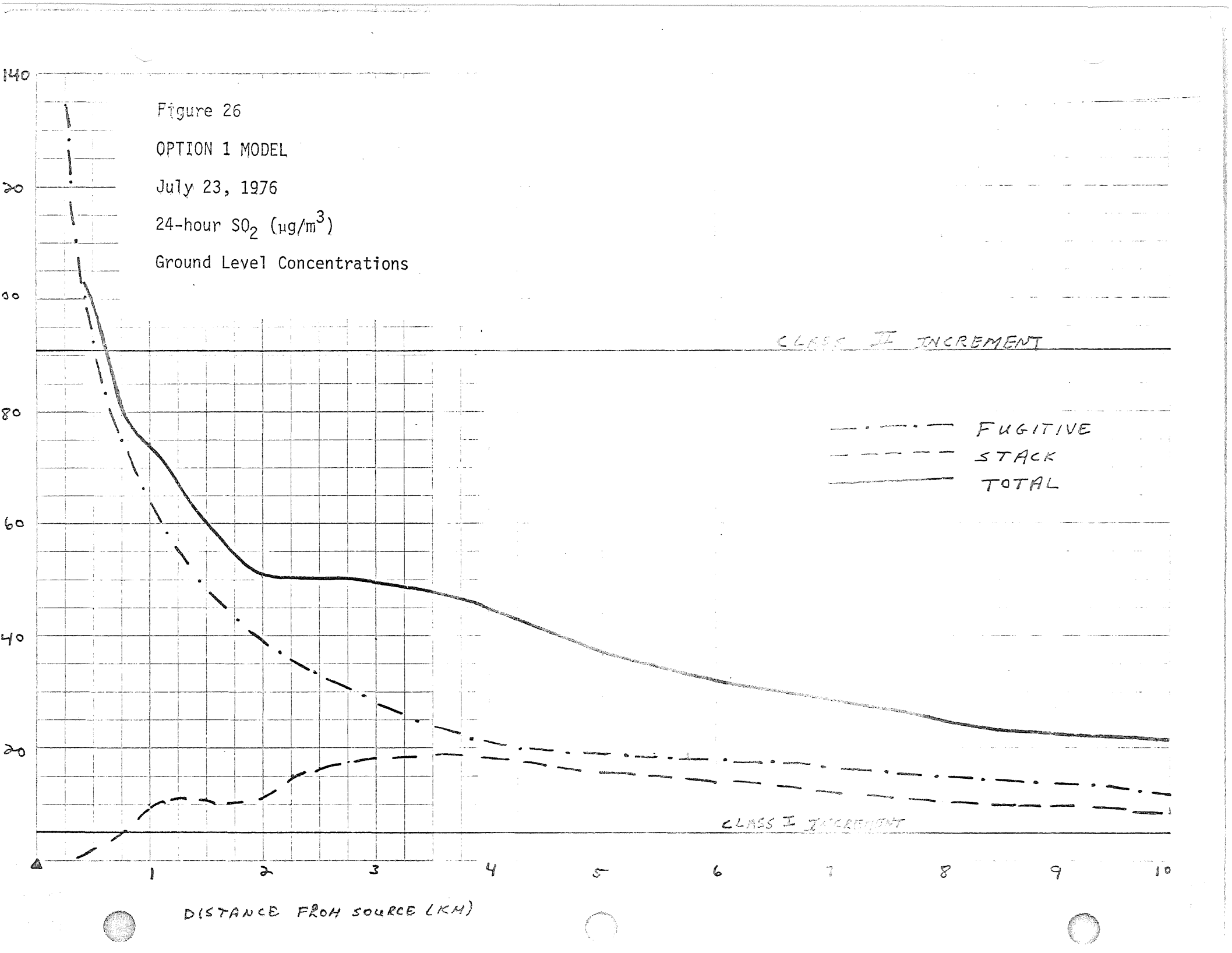
Figure 26
OPTION 1 MODEL
July 23, 1976
24-hour SO_2 ($\mu g/m^3$)
Ground Level Concentrations
140
120
100
80
60
40
20
CLASS II INCREMENT
FUGITIVE
STACK
TOTAL
CLASS I INCREMENT
1
2
3
4
5
6
7
8
9
10
DISTANCE FROM SOURCE (KM)

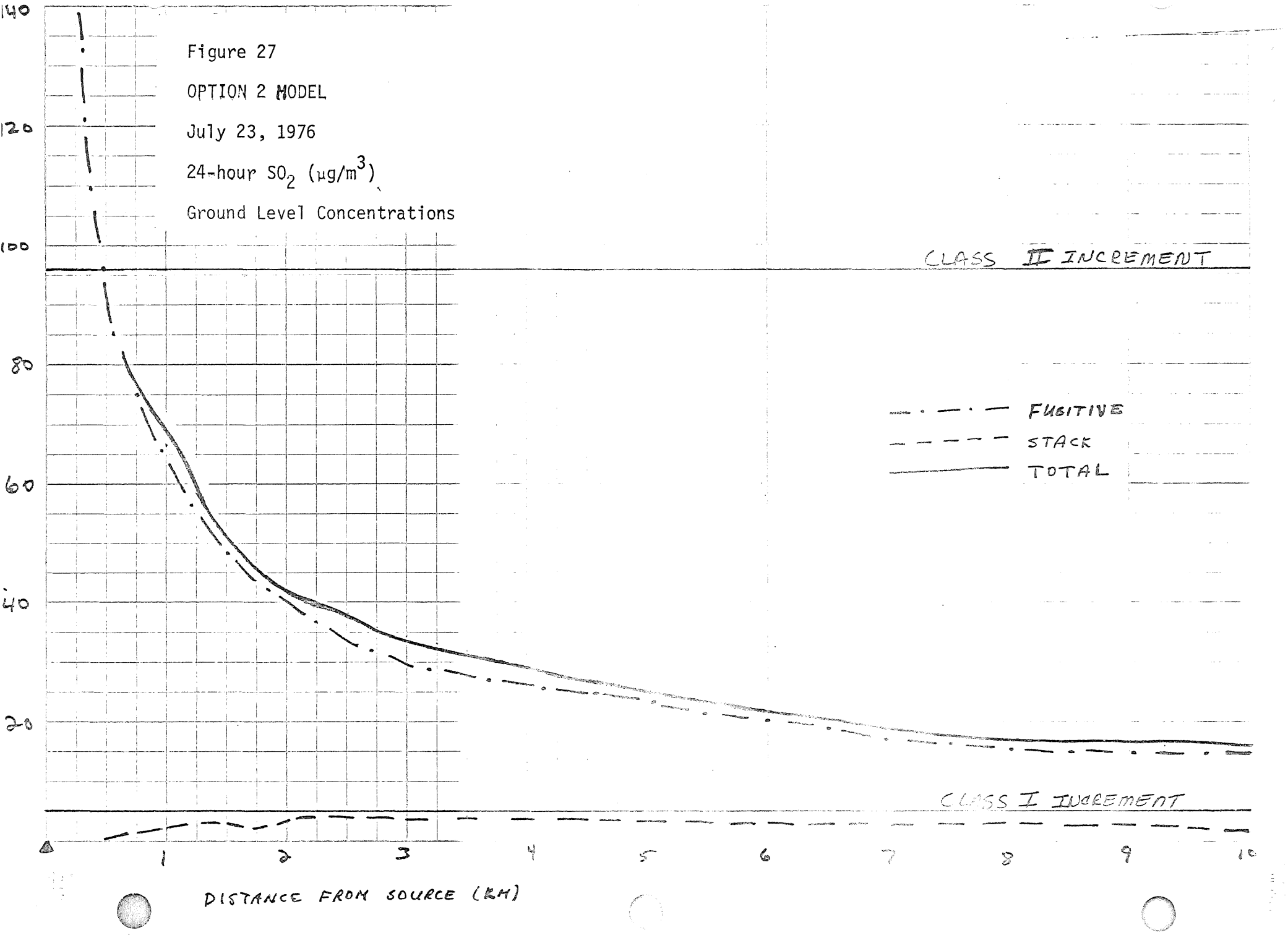
Figure 27
OPTION 2 MODEL
July 23, 1976
24-hour SO_2 ($\mu g/m^3$)
Ground Level Concentrations
140
120
100
80
60
40
20
CLASS II INCREMENT
FUGITIVE
STACK
TOTAL
CLASS I INCREMENT
1
2
3
4
5
6
7
8
9
10
DISTANCE FROM SOURCE (KM)

Figure 28

High Fugitive Basic Model

October 30, 1977

24-hour SO_2 ($\mu g/m^3$)

Ground Level Concentrations

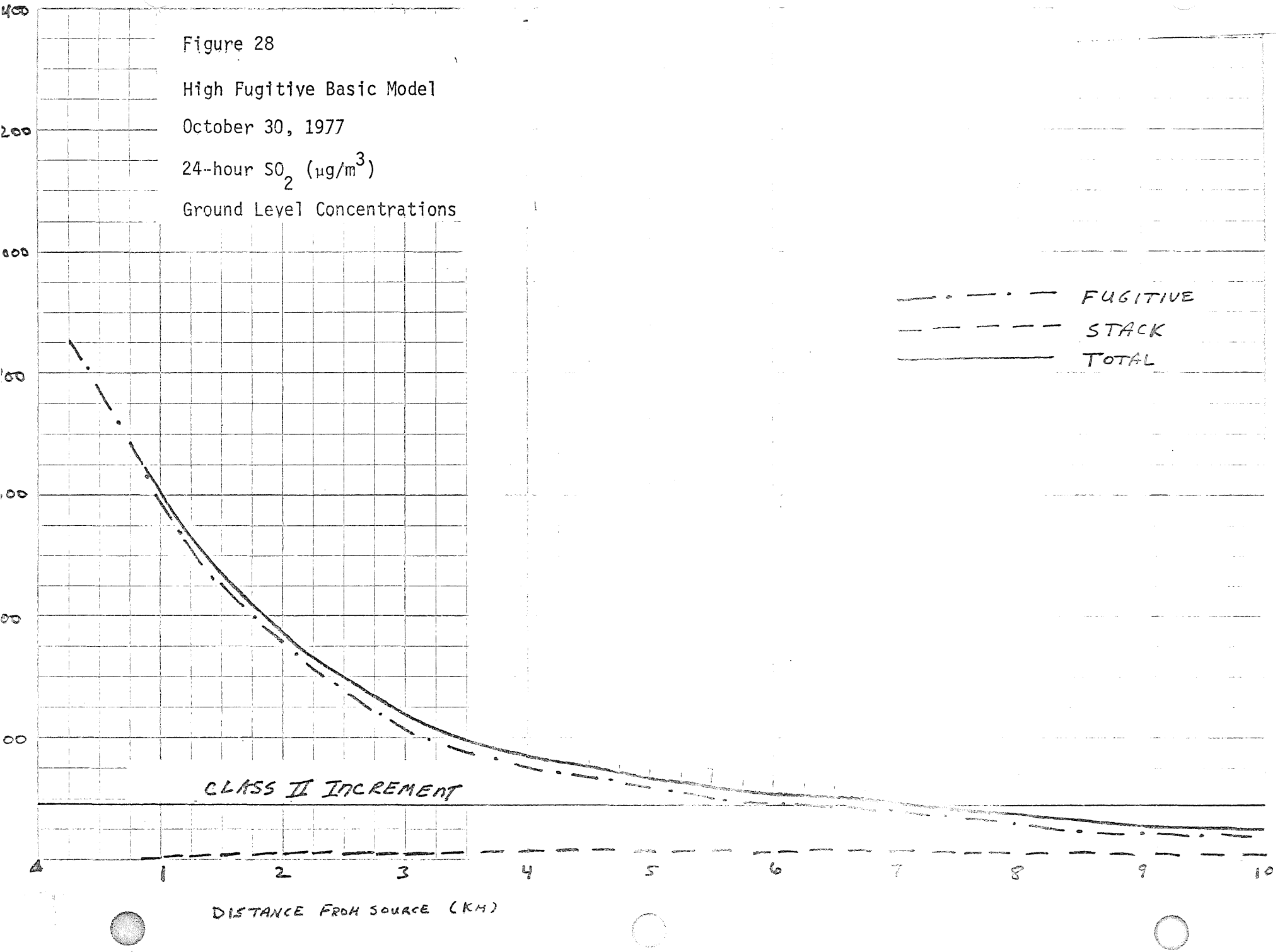

Figure 29

OPTION 1 MODEL

October 30, 1977

24-hour SO_2 ($\mu g/m^3$)

Ground Level Concentrations

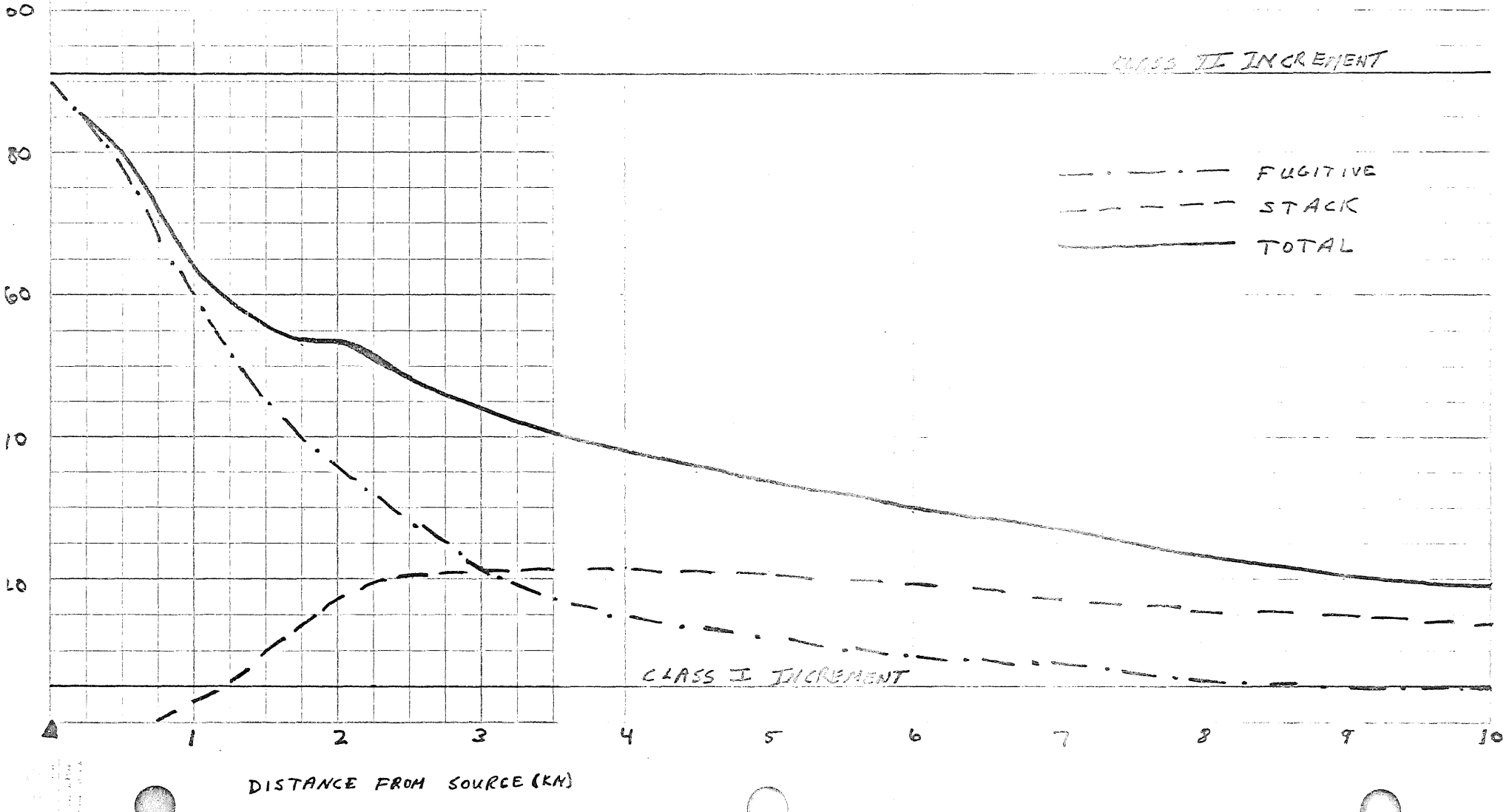

Figure 30

OPTION 2 MODEL

October 30, 1977

24-hour SO_2 ($\mu g/m^3$)

Ground Level Concentrations

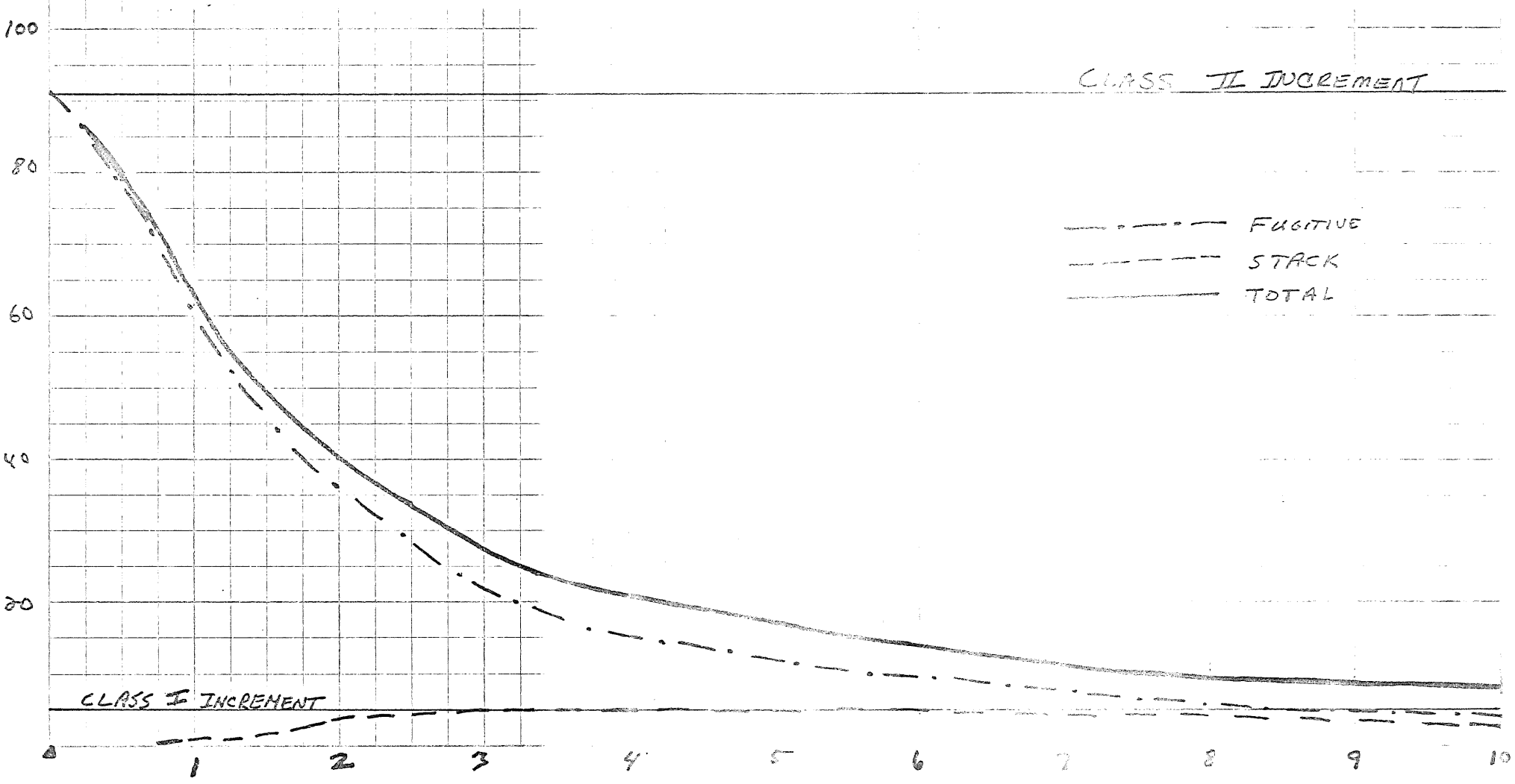

FIGURE 31

WIND ROSE
ANNUAL

HIBBING
1964–1973

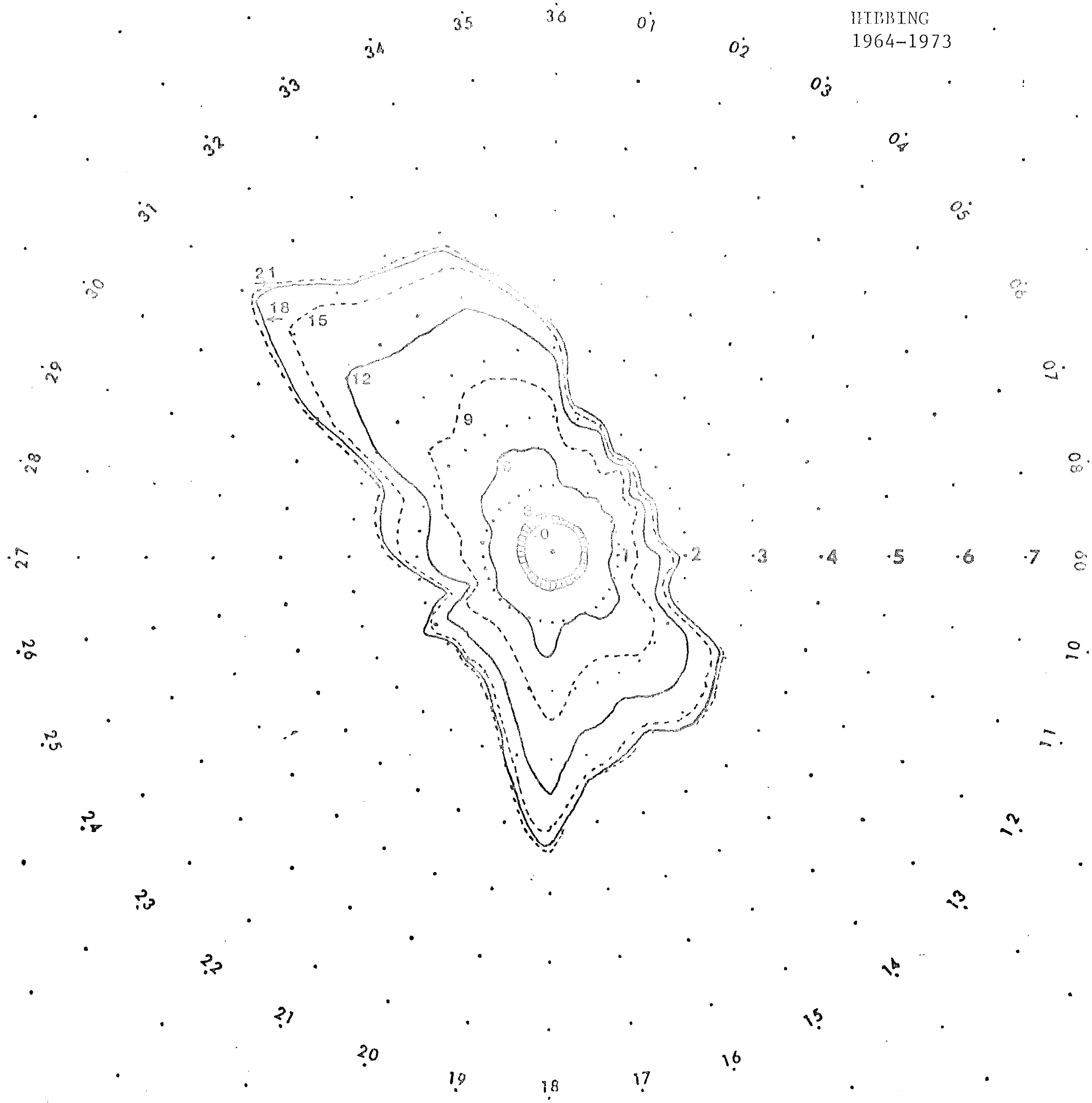

The various isopleths are for wind speeds in knots as labeled.

Source: Watson (1978b)

FIGURE 32

TOTAL NUMBER OF OCCURRENCES OF PERSISTENCE OF WIND DIRECTION AT THE HIBBING AIRPORT DURING THE PERIOD NOVEMBER 1, 1976 THROUGH OCTOBER 31, 1977

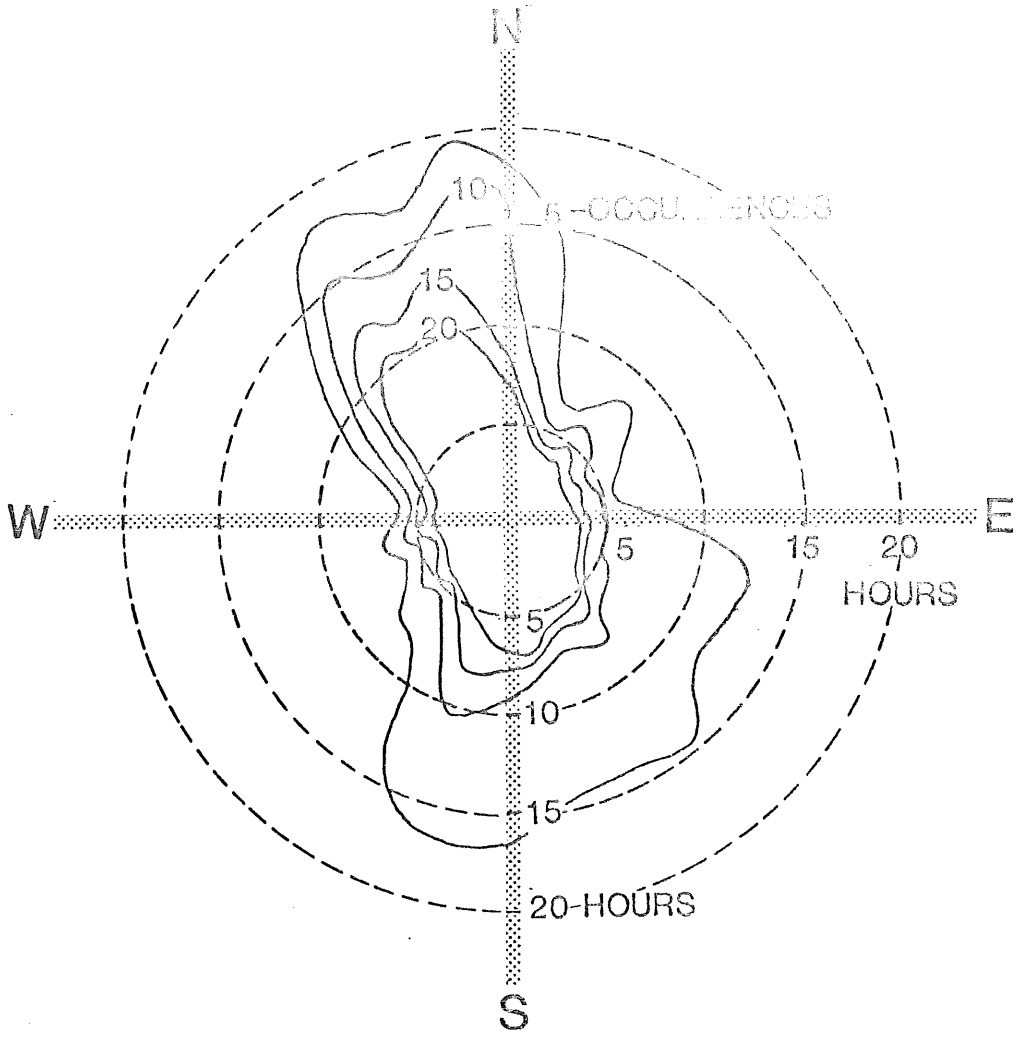

SOURCE : ENDERSEN, 1979

Figure 33

3-hour Case #1

Maximum SO_2 Concentrations

Base Case

Stability B

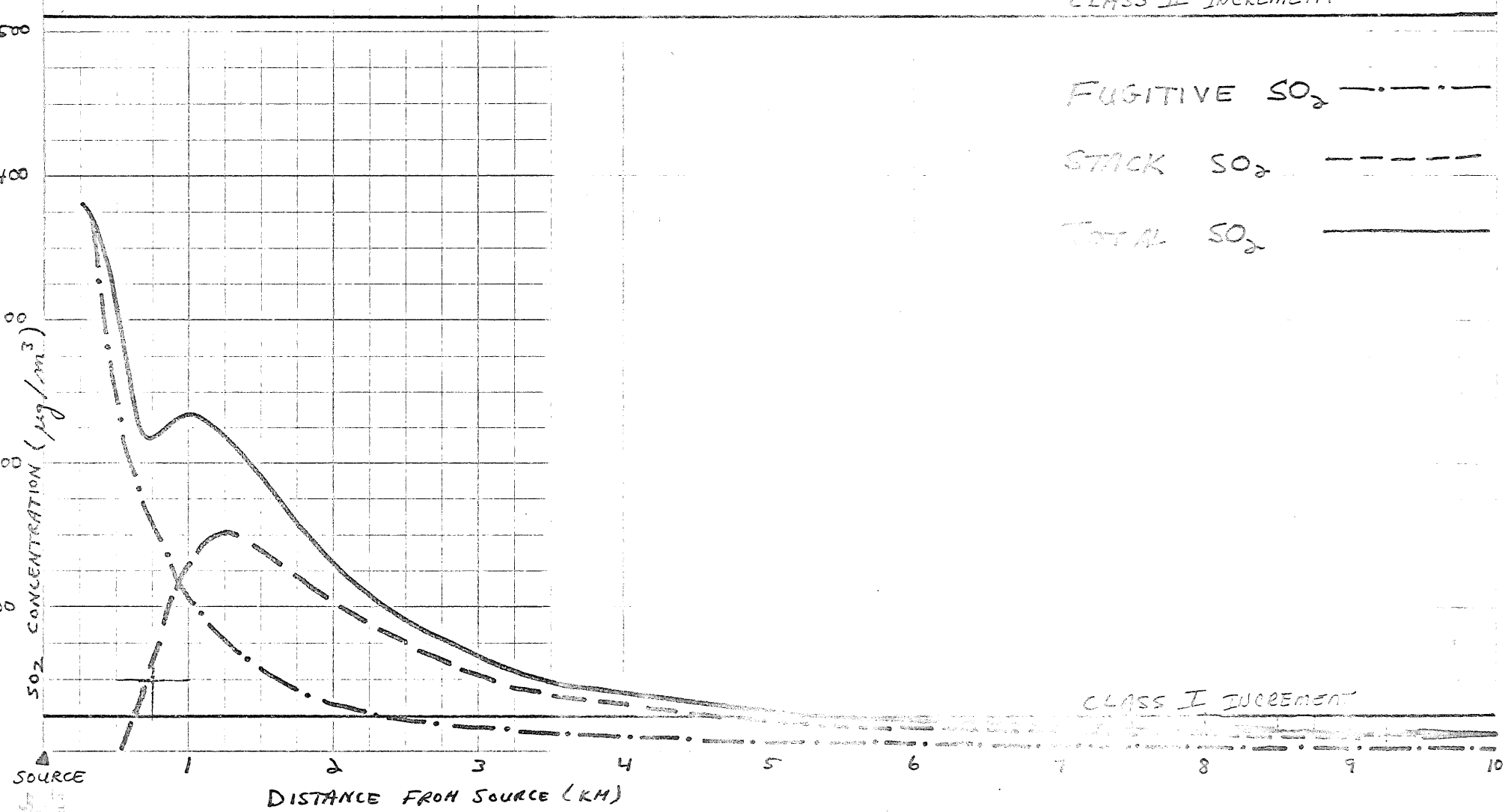

Figure 34

3-hour Case #3

Maximum SO_2 Concentrations

Base Case

Stability C

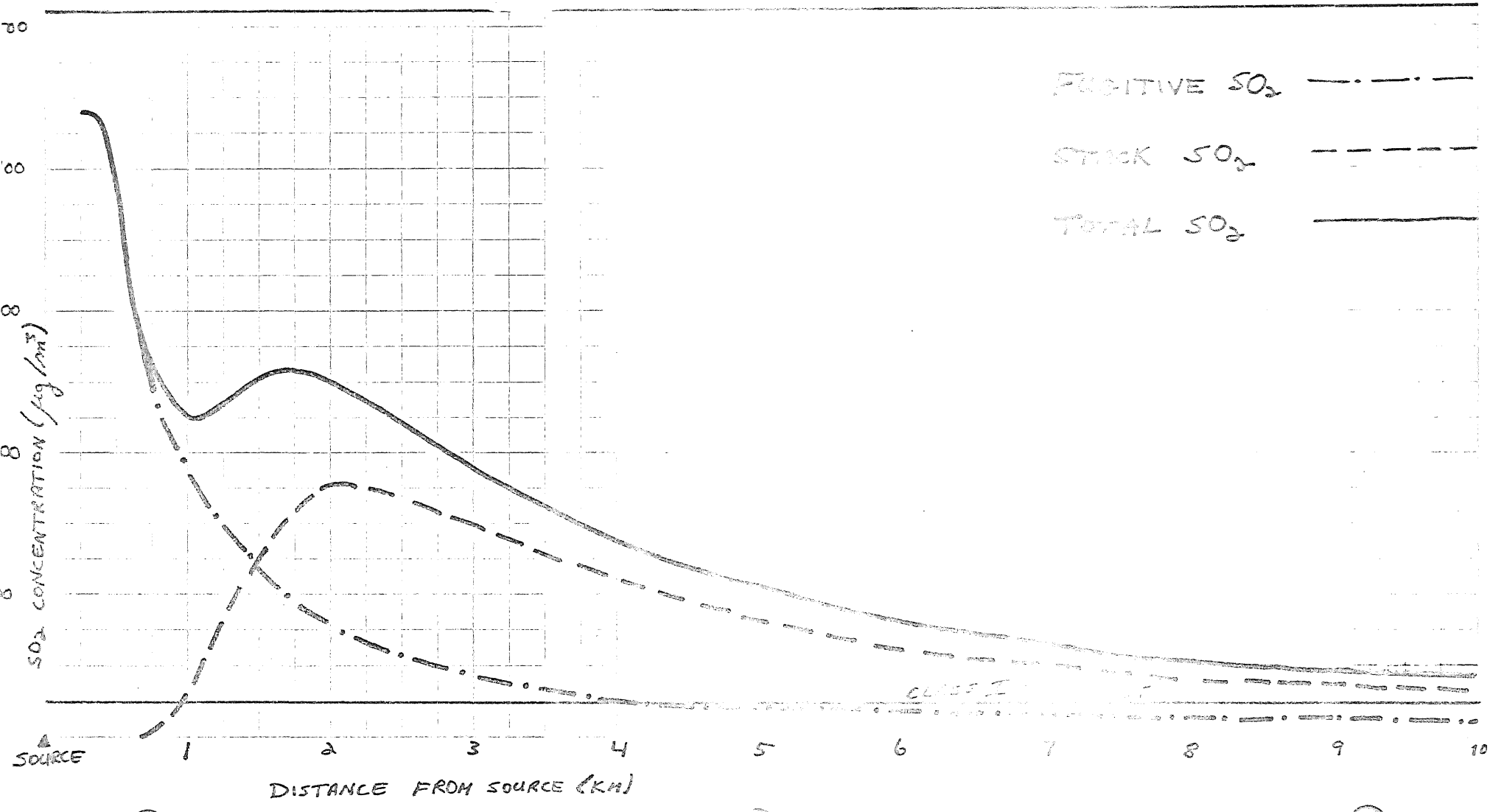

Figure 35

3-hour Case #9

Maximum SO_2 Concentrations

Base Case

Stability DD

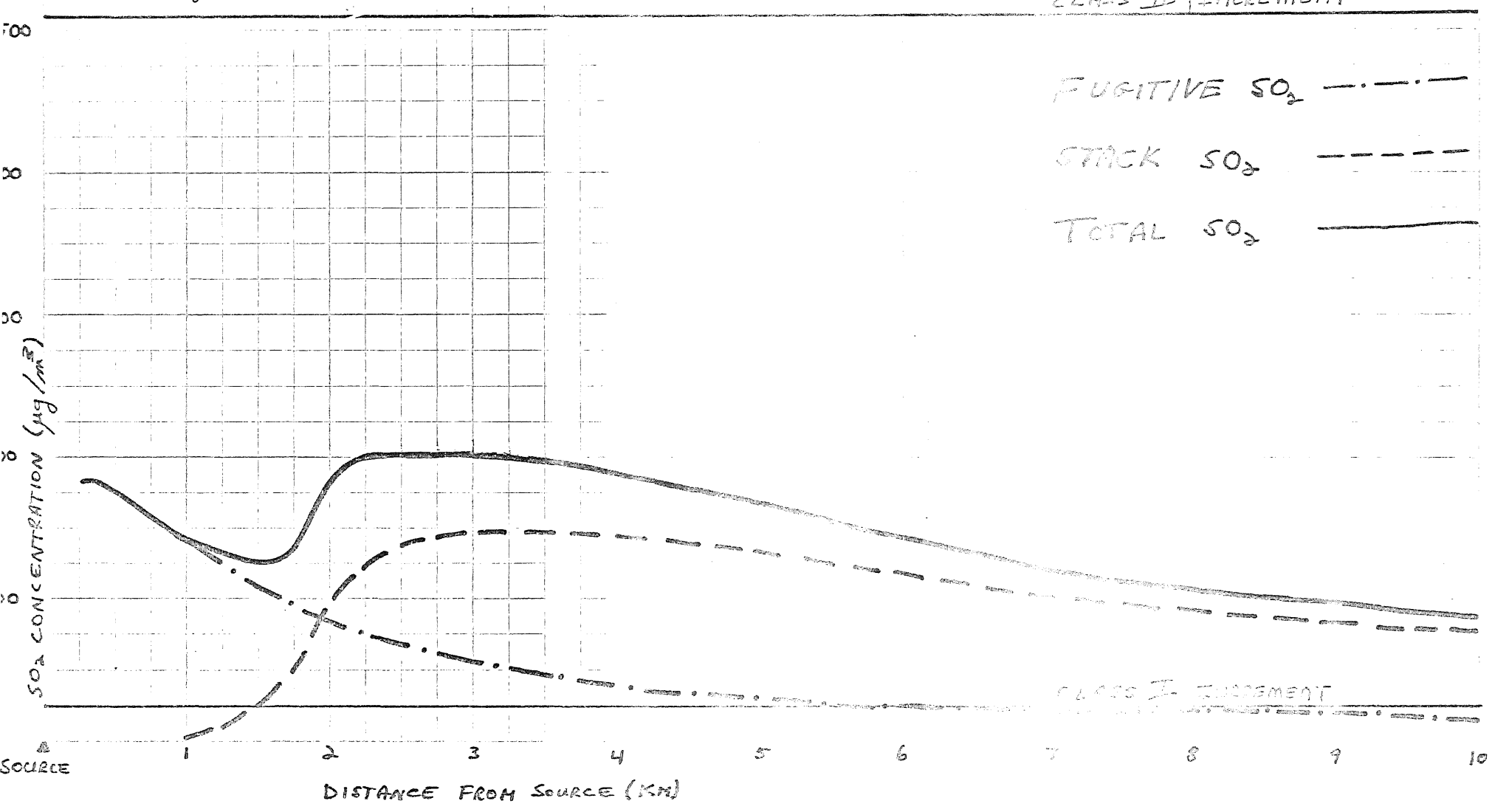

Figure 36

3-hour Case #10

Maximum SO_2 Concentrations

Base Case

Stability E

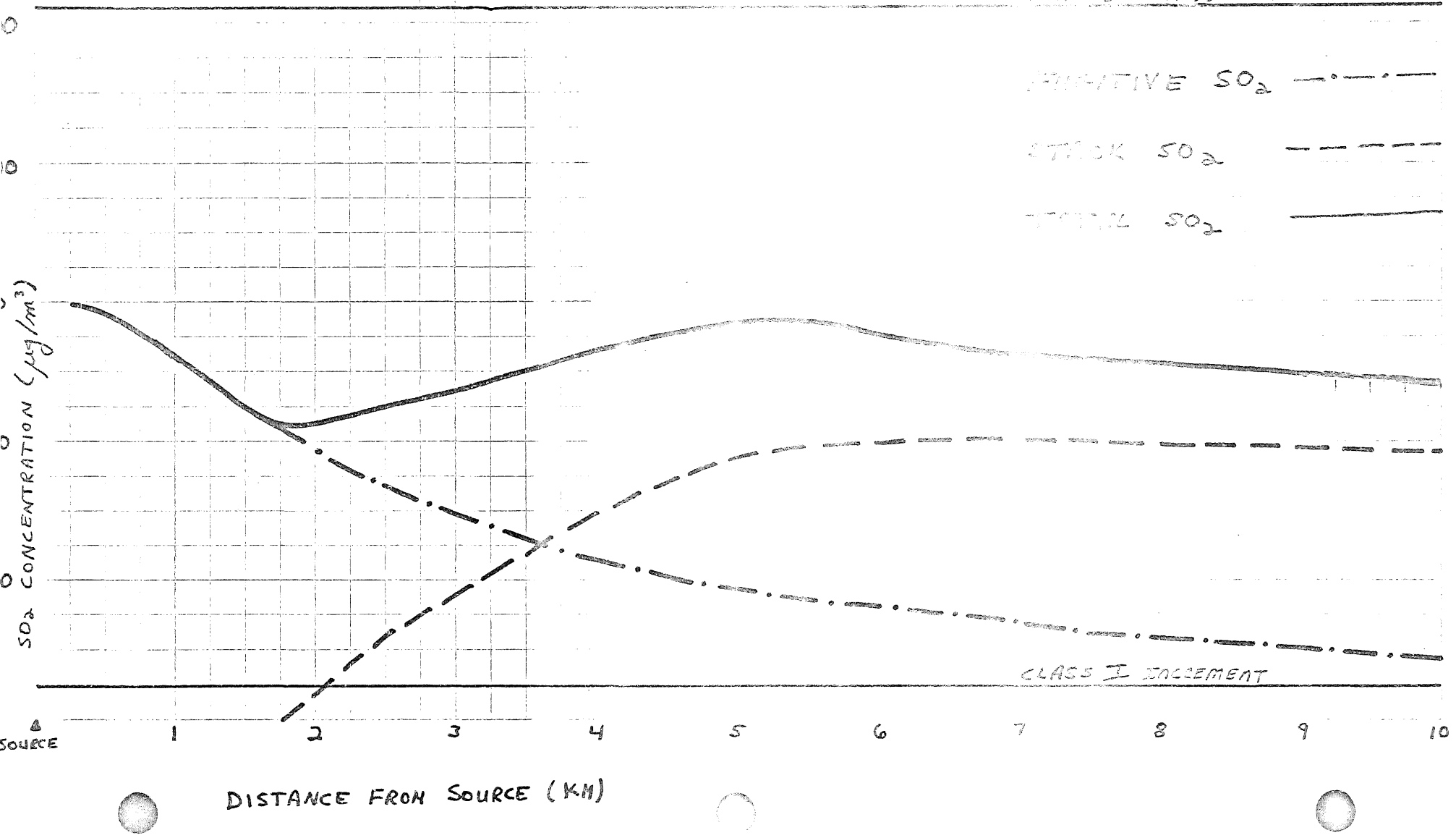

Figure 37

3-Hour Case #1

Maximum SO_2 Concentrations

Base Case

Stability F

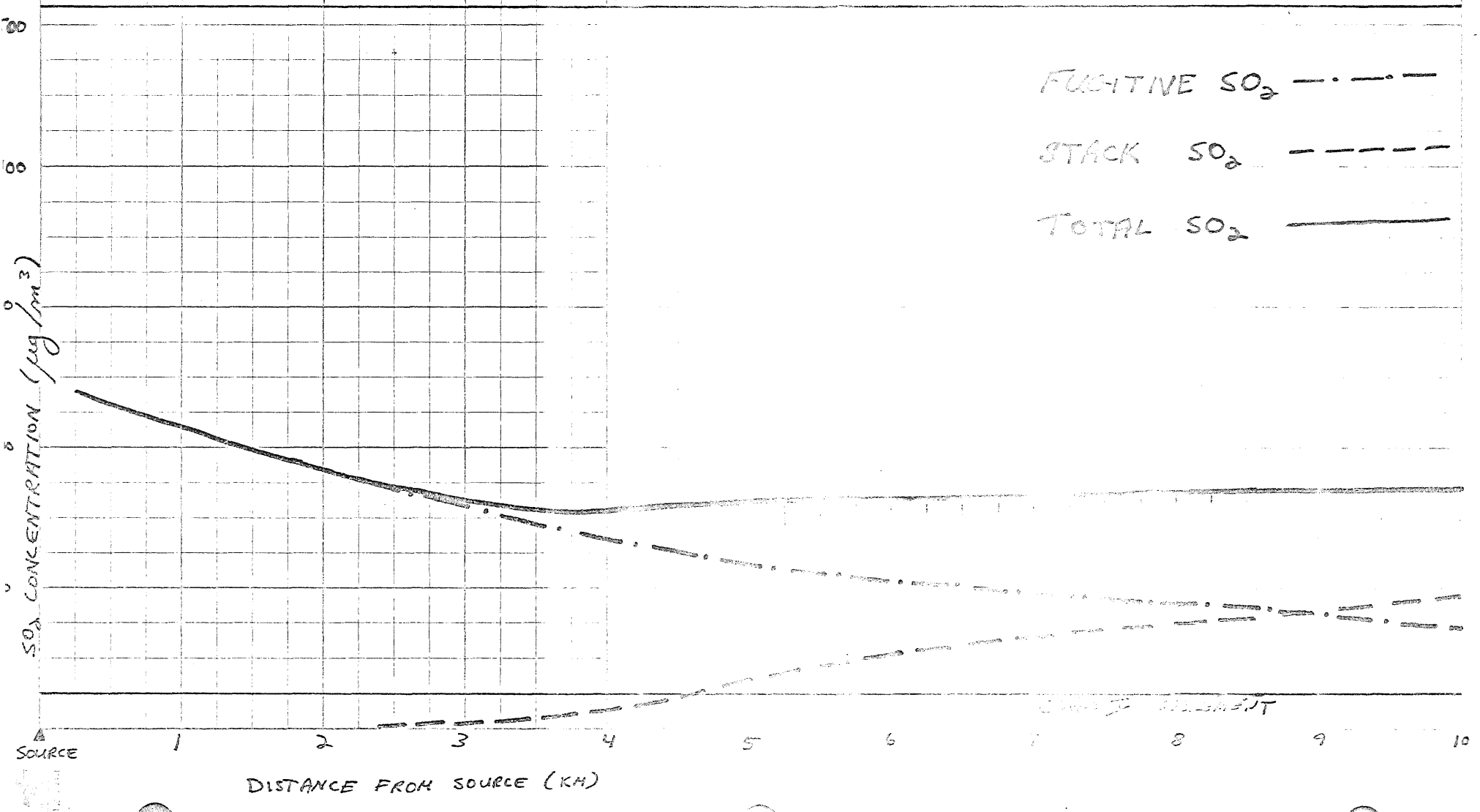

FIGURE 38

PREDICTED ANNUAL AVERAGE SO_2 CONCENTRATIONS FOR THE BASE CASE SMELTER WITH THE CLIMATOLOGICAL DISPERSION MODEL* (UG/M^3)

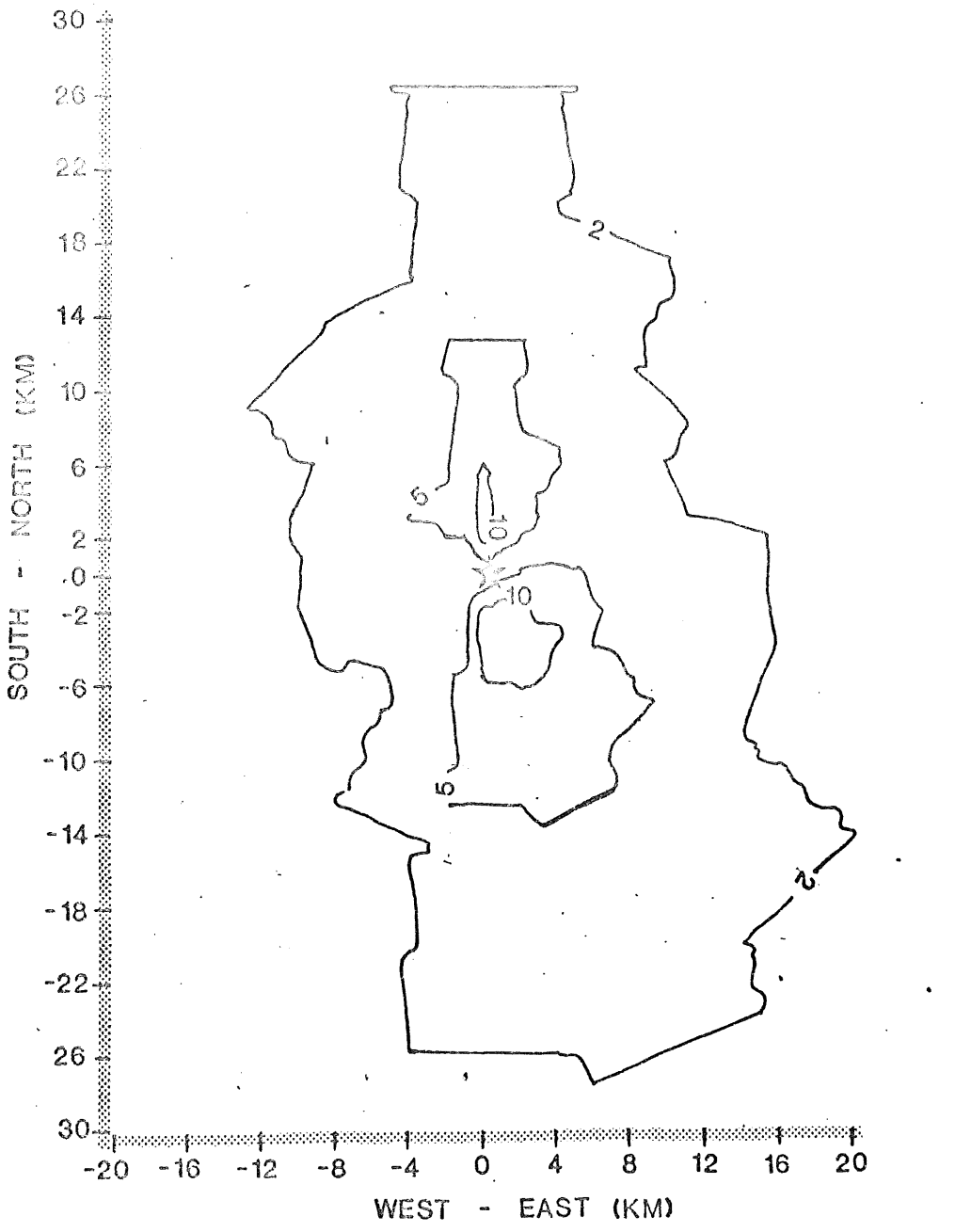

*BASED ON 1976 HIBBING WIND DATA

FIGURE 39

PREDICTED ANNUAL AVERAGE SO_2 CONCENTRATIONS FOR THE OPTION 2 SMELTER WITH THE CLIMATOLOGICAL DISPERSION MODEL* (UG/M3)

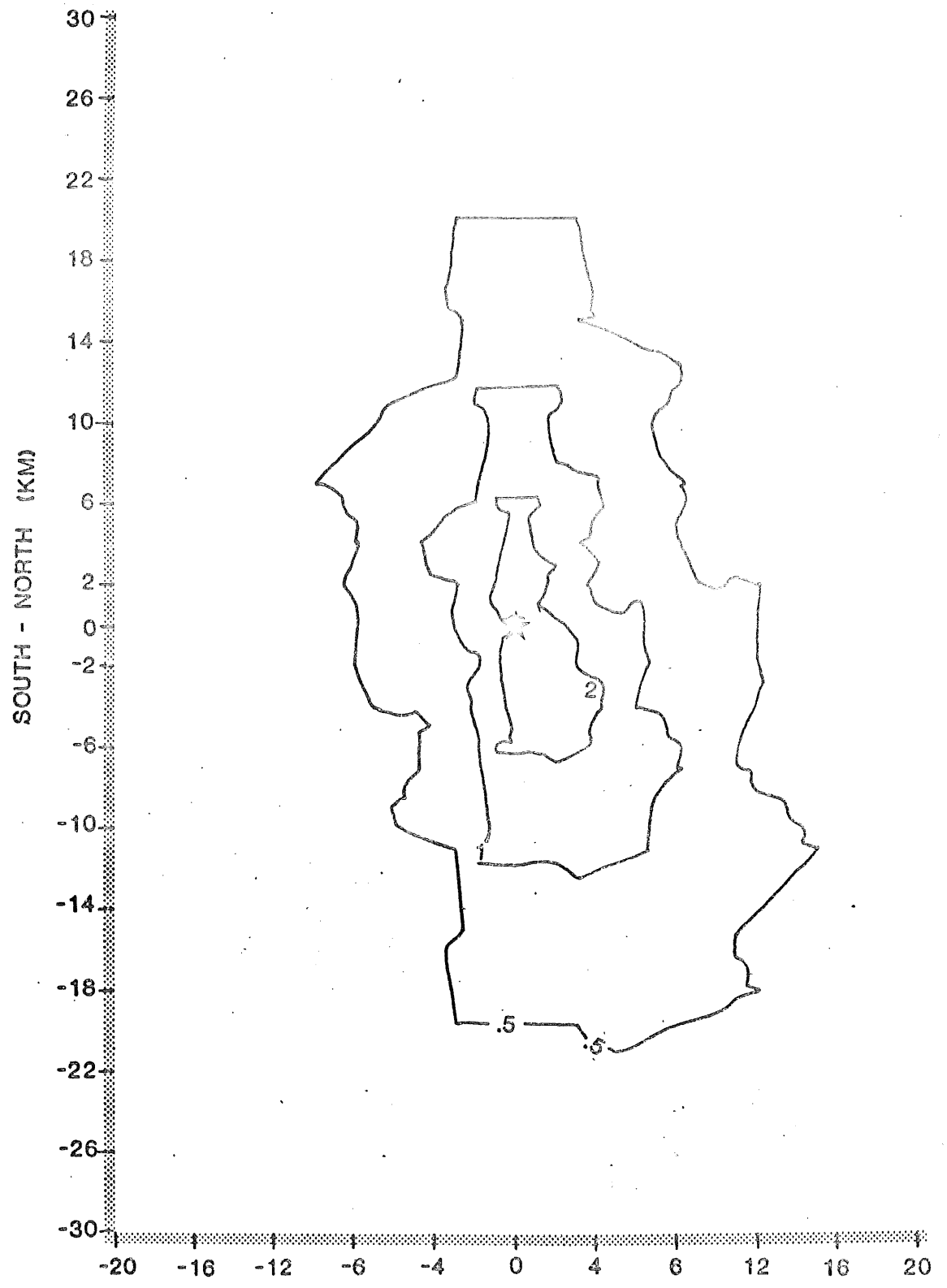

*BASED ON 1976 HIBBING WIND DAT

Figure 40

SO_2 Upset Case

Stack Release

3-hour Case #3

Slightly unstable

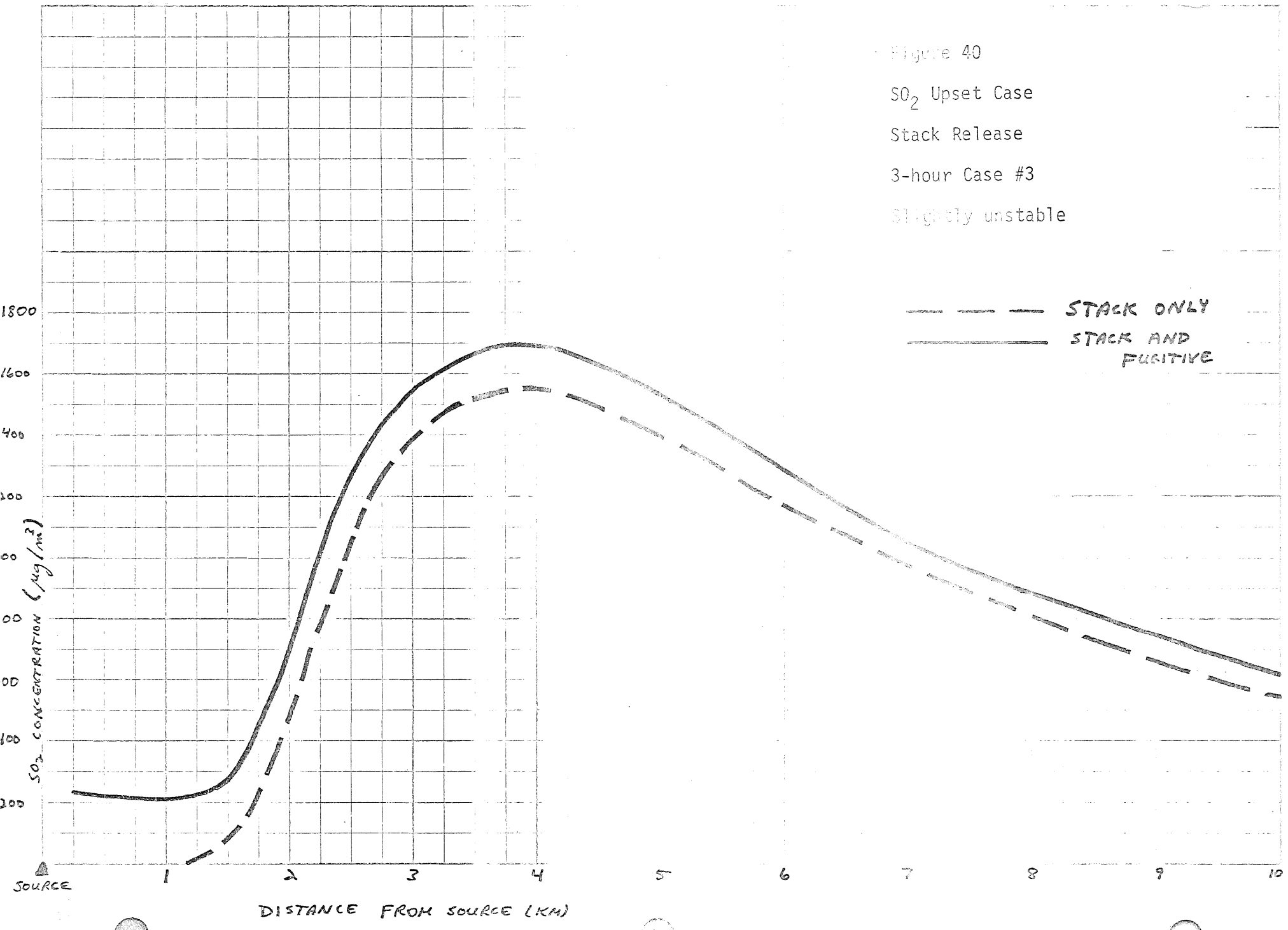

Figure 41

SO_2 Upset Case

Fugitive Release

3-hour Case #1

Very stable

STACK AND FUGITIVE

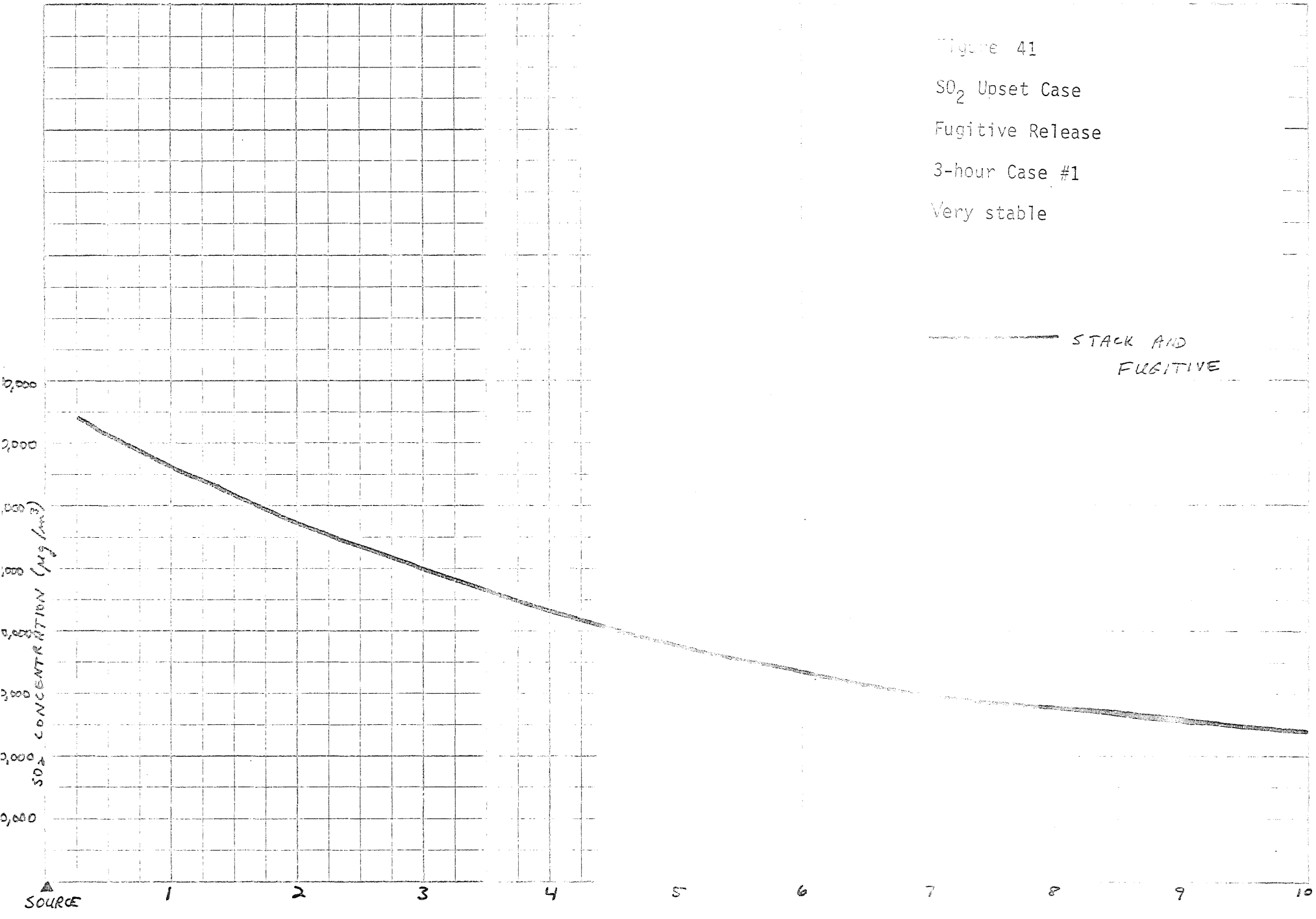

Table 1

Modeled Annual SO_2 Emissions* (metric tons per year)

Case	Stack	Fugitive
Base	11,284	990
High Fugitive (Basic Model)	2,354	9,920
Option 1	4,512	990
Option 2	1,002	990

Table 2

Modeled SO_2 Emission Rates (gm/sec)

	Short Term		Annual	
Case	Stack	Fugitive	Stack	Fugitive
Base	373	33	357	31
High Fugitive (Basic Model)	78	328	75	315
Option 1	149	33	143	31
Option 2	33	33	32	31

*Based on a model flash smelter producing 100,000 MTPY of copper and nickel metal, under normal operating conditions (see volume 2, chapter 4).

Table 3

Wind speed adjustment to pollutant release height

$$u\{H\} = u_o \left(\frac{H}{z_o}\right)^p$$

where $u\{H\}$ = wind speed at pollutant release height H

u_o = wind speed measured at height z_o

p = stability-dependant exponent

values of p

Stability Class	CDM and TEM	Fugitive
A (very unstable)	.10	.10
B (moderately stable)	.15	.15
C (slightly unstable)	.20	.20
D (neutral)	.25	.25
E (slightly stable)	.30	.30
F (very stable)	.30	.35

TABLE 4

COMPUTED

SO_2 HALF-LIVES (hours)

FOR DISPERSION MODELING

Stability	TEM (stack model)		Fugitive model	
	Snow	No snow	Snow	No snow
B	18.4	5.1	9.0	2.4
C	18.4	5.2	9.0	2.4
D	18.9	5.7	9.1	2.5
E	20.8	8.1	9.6	3.0
F	28.4	17.4	11.6	5.2

TABLE 5

Input Meteorology for March 14, 1976

Time Period	Time of Day	Stability Class	Wind Speed (m/sec)	Wind Direction	Temp (^{o}C)	Mixing Height (m)
1	0000 to 0300	D (night)	6.7	310	- 6	700
2	0400 to 0600	D (night)	6.2	300	-10	550
3	0700 to 0900	D (day)	6.9	307	-11	600
4	1000 to 1200	D (day)	7.6	317	- 7	1100
5	1300 to 1500	D (day)	8.1	317	- 5	1400
6	1600 to 1800	D (day)	8.6	310	- 6	1400
7	1900 to 2100	D (night)	6.0	307	-10	1200
8	2200 to 2400	E	4.8	290	-13	900

*At Hibbing Airport. Source: Federal Aviation Adminstration Flight Service Station.

TABLE 6

Input Meteorology for July 23, 1976

Time Period	Time of Day	Stability Class	Wind Speed (m/sec)	Wind Direction	Temp (^{o}C)	Mixing Height (m)
1	0000 to 0300	F	1.7	300	16	400
2	0400 to 0600	D (night)	3.9	317	17	350
3	0700 to 0900	C	3.8	310	21	800
4	1000 to 1200	D (day)	5.5	293	24	1350
5	1300 to 1500	C	5.0	320	26	1700
6	1600 to 1800	D (day)	6.0	293	26	1400
7	1900 to 2100	D (day)	3.5	300	21	1000
8	2200 to 2400	E	3.3	303	16	600

Table 7
Input Meteorology for October 28, 1976

Time Period	Time of Day	Stability Class	Wind Speed (m/sec)	Wind Direction	Temp (°C)	Mixing Height (m)
1	0000 to 0300	D (night)	6.5	217	- 2	640
2	0400 to 0600	D (night)	5.8	210	- 2	580
3	0700 to 0900	D (day)	5.5	210	0	620
4	1000 to 1200	D (day)	7.7	220	6	900
5	1300 to 1500	D (day)	8.4	213	12	1100
6	1600 to 1800	D (day)	6.5	213	10	1000
7	1900 to 2100	E	5.6	227	7	850
8	2200 to 2400	E	3.1	200	4	700

TABLE 8

Input Meteorology for November 6, 1976

Time Period	Time of Day	Stability Class	Wind Speed (m/sec)	Wind Direction	Temp (°C)	Mixing Height (m)
1	0000 to 0300	D (night)	6.4	310	0	640
2	0400 to 0600	D (night)	7.2	320	-1	580
3	0700 to 0900	D (day)	8.0	323	-2	600
4	1000 to 1200	D (day)	7.7	320	0	900
5	1300 to 1500	D (day)	7.2	327	0	1100
6	1600 to 1800	D (day)	5.6	330	-3	1100
7	1900 to 2100	D (night)	7.2	323	-5	850
8	2200 to 2400	E	5.6	330	-7	700

TABLE 9

Input Meteorology for December 20, 1976

Time Period	Time of Day	Stability Class	Wind Speed (m/sec)	Wind Direction	Temp (^{o}C)	Mixing Height (m)
1	0000 to 0300	D (night)	6.9	330	-20	510
2	0400 to 0600	D (night)	7.4	347	-22	480
3	0700 to 0900	D (night)	7.0	337	-24	470
4	1000 to 1200	D (day)	6.7	350	-22	600
5	1300 to 1500	D (day)	8.2	330	-19	650
6	1600 to 1800	D (day)	6.2	340	-20	630
7	1900 to 2100	E	5.1	347	-22	600
8	2200 to 2400	E	4.4	350	-24	560

TABLE 10

Input Meteorology for January 15, 1977

Time Period	Time of Day	Stability Class	Wind Speed (m/sec)	Wind Direction	Temp (^{o}C)	Mixing Height (m)
1	0000 to 0300	E	4.8	313	-28	510
2	0400 to 0600	E	3.9	317	-30	480
3	0700 to 0900	E	4.9	323	-23	470
4	1000 to 1200	D (day)	5.8	333	-28	600
5	1300 to 1500	D (day)	7.2	323	-26	650
6	1600 to 1800	D (day)	6.7	330	-27	630
7	1900 to 2100	D (night)	6.0	323	-30	600
8	2200 to 2400	E	4.8	327	-31	560

TABLE 11

Input Meteorology for February 28, 1977

Time Period	Time of Day	Stability Class	Wind Speed (m/sec)	Wind Direction	Temp (^{o}C)	Mixing Height (m)
1	0000 to 0300	F	2.9	340	-13	700
2	0400 to 0600	F	2.1	330	-15	550
3	0700 to 0900	D (day)	4.1	327	-14	520
4	1000 to 1200	D (day)	5.7	330	-10	800
5	1300 to 1500	D (day)	6.7	323	- 6	1100
6	1600 to 1800	D (day)	6.4	340	- 7	1150
7	1900 to 2100	D (night)	5.1	330	-10	1100
8	2200 to 2400	E	5.5	327	-12	850

TABLE 12

Input Meteorology for October 30, 1977

Time Period	Time of Day	Stability Class	Wind Speed (m/sec)	Wind Direction	Temp (^{o}C)	Mixing Height (m)
1	0000 to 0300	D (night)	4.4	150	9	640
2	0400 to 0600	D (night)	4.6	150	9	580
3	0700 to 0900	D (day)	6.7	160	9	600
4	1000 to 1200	D (day)	8.6	153	10	900
5	1300 to 1500	D (day)	8.4	153	12	1100
6	1600 to 1800	D (day)	7.2	153	9	1000
7	1900 to 2100	D (night)	7.6	147	9	850
8	2200 to 2400	D (night)	7.6	150	9	700

Table 13

3-hour Dispersion Meteorology

Case #	Stability Class	Windspeed (m/sec)	Temp (°C)	Mixing Ht (m)
1*	B	2	30	1500
2	B	3	30	1500
3*	C	2	30	1500
4	C	4	30	1500
5	C	6	30	1500
6	DD	6	25	1500
7	DD	8	25	1500
8	DN	4	20	200
9*	DD	4	25	1500
10*	E	2	20	200
11*	F	2	15	200

DD=Neutral day

DN=Neutral night

*Results presented for these cases

Table 14

Modeled 3-hour SO_2 concentrations

Base Case

Maximum concentrations (downwind-peaks)*

Case #	Stability	Maximum concentration ($\mu g/m^3$)	Distance (km)
1	B	233	1.1
3	C	254	1.8
9	DD	202	2.8
10	E	281	5.0
11	F	164	9.2

*based on the TEM and the Fugitive Model.

APPENDIX

PLUME DISPERSION CONSIDERATIONS FOR SMELTER SITING IN NORTHEASTERN MINNESOTA

I. Introduction

The dispersion pattern of a plume in the atmosphere is determined basically by the wind speed and direction, the rates of vertical and horizontal mixing, and the limits to vertical and horizontal mixing. The following is a brief summary of these three factors and their relative importance in several potential copper-nickel smelter site areas in northeastern Minnesota.

II. The Mechanisms of Dispersion

The initial dilution and advective movement of the plume is controlled by the transport wind; that is, the wind blowing at plume height. As a waste gas stream is injected into the atmosphere, it undergoes an initial dilution proportional to the wind speed. The plume centerline then follows the wind streamlines at the height of final plume rise (ignoring gravitational settling and bouyancy effects).

Plumes mix with ambient air (i.e., disperse), therefore reducing their pollutant concentrations, and are brought to the ground by turbulence and molecular diffusion. Molecular diffusion is a very slow process, is negligible except for extremely stable atmospheres, and will not be considered in this discussion. Most dispersion is caused by turbulence and is generated by thermal or mechanical mechanisms.

Thermal Turbulence

Thermal instability results from solar heating of the ground and, by conduction and convection, the lower atmosphere. This instability is released as

turbulence when bubbles of warm air rise, cooler air aloft sinks, and the plume is mixed by the turbulent eddies. The classic diurnal pattern is completed under clear skies at night when the lowest layers cool rapidly by radiation, the atmosphere becomes stable (i.e., resistant to vertical displacements), and little mixing occurs. An atmosphere of neutral stability exists between these extremes when daytime overcast conditions prevent significant surface heating, when night-time overcase conditions prevent significant surface cooling, or when wind with speeds greater than about 5 m/sec mix the atmosphere. Because neutral stability typically does not follow a diurnal cycle, it is usually the most persistent type of stability. Atmospheric thermal instability generally decreases with height, and the atmosphere becomes more neutral aloft. Thermal stability, however, often remains high throughout a surface-based or elevated temperature inversion layer (i.e., layer in which temperature increases with height).

Mechanical Turbulence

Mechanical turbulence is generated by air flow over obstructions such as buildings, terrain features, and vegetation and by changing wind velocity with height (wind shear). Mechanical turbulence causes forced mixing of the atmosphere, enhances the mixing effects of thermal instability while decreasing the lapse rate, reduces thermal stability, and generally drives the atmospheric thermal structure toward an adiabatic state.

Lakeshore Effects

During the warm season daytime, lakes are cooler and aerodynamically more flat than the land, and the air over them is usually very stable. Elevated plumes emitted along lakeshores during stable onshore flow (daytime lake breeze or large scale onshore flow) often remains quite concentrated until they

intersect the turbulent internal boundary layer (TIBL) and then are mixed rapidly to the surface. This lakeshore fumigation regime can cause persistent high pollutant concentrations within the TIBL.

Another important feature of lakeshore transport occurs during persistent offshore flow over cold lakes. Plumes enter the stable offshore regime and have excellent potential for long distance transport.

Urban Effects

Urban areas contribute thermally and mechanically to the instability of their own atmospheres. Heat emitted from buildings and vehicles and sunlight absorbed and emitted as heat by dark pavement and buildings all enhance the daytime unstable atmosphere and prevent low level inversions from forming at night. Urban buildings also produce mechanical turbulence whenever the wind blows past them.

Limits to Mixing

Finite limits to mixing do exist. Neutral and unstable plumes typically disperse vertically until they become trapped between the ground and the top of the mixed layer (often an inversion) at a height of typically 500 to 3000 meters. With continued travel downwind, the plume becomes more uniformly dispersed throughout the mixed layer. Stable plumes, especially those trapped in an inversion, exhibit little dispersion and can remain aloft with high concentrations of pollutants.

Horizontal dispersion can be limited by the channeling of the flow by valleys or by impingement of the plume on hills and ridges. Unstable flows usually respond to the displacement and flow with the streamlines over a ridge without impingement on the surface by the plume centerline. Stable flows generally resist the displacement, impact the ridge, and try to flow around it. Weak

stable flows that cannot pass the ridge can become trapped and, if persistent, can lead to very high pollutant concentrations. This air stagnation/terrain trapping situation has led to history's worst air pollution episodes. A terrain feature upwind of a source, however, can enhance dispersion through increased turbulence, flow splitting, and plume meander.

Another type of topographic trapping in hilly terrain occurs on calm, clear nights when cool air drains downhill into valleys and traps pollutants in pools of very stable air. The reverse situation occurs during sunny days when heated air flows up the hills and increases pollutant dispersion. Upslope winds are generally much weaker than downslope winds.

III. Dispersion Considerations for Potential Smelter Sites

Several areas of northeastern Minnesota may be considered for copper-nickel smelter siting. General dispersion conditions for these areas are discussed here and are summarized in the table at the end of this appendix. It cannot be stressed too strongly that these are preliminary estimates only, based on general insight and on non-Minnesota data rather than on on-site field data.

Babbitt Area

One of the most likely areas for a smelter site is near the copper-nickel resource area, a few kilometers south of the Iron Range. The Range probably has little effect on low level turbulence along the Duluth gabbro contact, and unstable flow approaching the Range should flow over it with little variation from the flat terrain case. A stable plume being blown with the frequent southeasterly winds, however, would impinge on the Range and try to flow around it or through gaps. Stable conditions and low wind speeds could lead to a significant pollutant buildup south of the Range. The Iron Range is also expected to cause diversion of low level winds, nighttime thermal drainage flows, and daytime upslope flows. Upslope flows may be especially important

for early morning inversion breakup and plume dispersion on the south side of the Range because it faces the morning sun.

Local terrain south of the Range is mostly gently rolling and should have little effect on plume dispersion. Isolated hills, such as the eighty-foot hill near the AMAX test shaft, exist, however. Wind blowing across the hill and toward the smelter could cause enhanced local turbulence or aerodynamic downwash. Wind blowing a smelter plume toward such a hill could lead to impingement of the plume on the hill.

The area north of the Iron Range is fairly flat and would experience dispersion phenomena similar to those found south of the Range. The primary difference is that the prevailing cold northwesterly winds impinge on the steep north side of the Range and terrain trapping could cause high concentrations. Daytime upslope flow is much weaker on the north side of the Range because it is steeper than the south side and faces away from the sun. As with the region south of the Range, local effects of hills can be significant.

A smelter plume emitted at the top of the Iron Range would experience higher wind speeds, greater initial dilutions, and fewer local deflections than a plume emitted a few kilometers to the north or south. A plume emitted near the top of a ridge, however, can become involved in a number of lee wave phenomena such as downwash, streamline compression and expansion, down-wind surface impingement, enhanced plume meander, thermal drainage flows into nearby valleys, and daytime upslope flows.

Lake Superior North Shore

The Lake Superior North Shore region offers several potential smelter sites. This region suffers from combined lakeshore and topographic restrictions to dispersion. The frequent stable southeasterly lake breezes in summer

provide a vertical limit to mixing and would trap pollutants in the TIBL over the land. The high bluffs parallel to the lake not only deflect low level winds along a more northeast-southwest axis, but provide a limit to downwind travel and a potential area for terrain impingement. The bluffs also cause nighttime drainage flows that could transport a plume away from the source and offshore over Lake Superior where it could stagnate until morning and then flow back onshore with the lake breeze. Polluted air could slosh back and forth for days before complete dispersal by a frontal system or persistent strong winds. Plumes emitted in summer during persistent offshore flow would have considerable potential for long distance transport across the cold expanse of Lake Superior. The only beneficial feature of this area is that the ridge faces the rising sun and low level nocturnal inversions should break early in the day.

Duluth Area

The Duluth lakeshore/St. Louis River valley region is basically an extension of the North Shore region and exhibits similar dispersion phenomena of wind deflection, terrain impingement and trapping, drainage flows, lake breeze trapping and the potential for long distance transport. Because the bluffs terminate in Duluth, however, air tends to be channeled along the bluffs, southward along the St. Louis River, and over the open, flat terrain southwest of Duluth. These flow patterns are not well-understood. Another difference from the North Shore region is that the urban effect of Duluth enhances thermal and mechanical turbulence.

The Lake Superior bluffs region above the city of Duluth has generally good dispersion because of the relatively high wind speeds found there and the absence of topographic plume trapping features. Potential problems include nighttime drainage flows that could carry plumes into Duluth's downtown and residential areas and the threat of long distance transport over Lake Superior.

SUMMARY OF DISPERSION CONSIDERATIONS

	South Side of Iron Range	North Side of Iron Range	On Iron Range	North Shore	Duluth Lakeshore	Lake Superior Bluffs
Wind Speed	Moderate	Moderate	High	Moderate	Moderate	Moderate to high
Solar Radiation	High in morning	Low in morning	Moderate	High in morning	High in morning	Moderate
Terrain-Induced Turbulence	Generally small increase; potentially large locally	Generally small increase; potentially large locally	Moderate increase	Unknown	Unknown	Unknown
Urban Effect	None	None	None	Site-dependent	Moderate	Slight to Moderate
Lake Effect	None	None	None	Large	Large	Slight
Depth of Mixed Layer	Sometimes restricted	Sometimes restricted	Moderate	Often shallow	Often shallow	Moderate
Plume Channeling	Moderate	Moderate	Small	Moderate	Moderate	None
Terrain Impingement Or Trapping	Moderate	Large	Unknown	Moderate to large	Moderate to large	None
Drainage Flows	Moderate	Moderate	Unknown	Moderate	Moderate	Possibly significant
Upslope Flows	Moderate	Weak to Moderate	Unknown	Moderate	Moderate	weak to moderate

NOTE: These dispersion considerations are appraisals for discussion purposes only, and are subject to extensive revision after further study.